POGZ controls embryonic stem cell self-renewal and pluripotency by association with esBAF and HP1

Xiaoyun Sun[1#] Linxi Cheng[1,2#] Yuhua Sun[1,2,3*]

1, Institute of Hydrobiology, Chinese Academy of Sciences
2, University of Chinese Academy of Sciences
3, innovation of seed

#: these authors contribute equally; *: corresponding author

Email: sunyh@ihb.ac.cn

Abstract

POGZ, which encodes a multi-domain transcription factor, has been found frequently mutated in neurodevelopmental disorders, particularly autism spectrum disorder (ASD) and intellectual disability (ID). However, little is known about its function in ESC self-renewal and pluripotency, cell fate determination as well as in transcriptional regulation. Here, using embryonic stem cells (ESCs) as model, we show that POGZ plays key roles in the maintenance of ESC and cell fate determination by association with the SWI-SNW chromatin remodeler complex and heterochromatin protein 1 (HP1) proteins. POGZ is essential for the maintenance of ESC undifferentiated state, and loss of POGZ leads to ESC differentiation, likely by up-regulation of primitive endoderm and mesoderm lineage genes and by down-regulation of pluripotency-related genes. Mechanistically, POGZ may control ESC-specific gene expression by association with chromatin remodeler complex esBAF and HP1s, and they can form a PBH triplex. POGZ functions primarily to maintain an open chromatin, as loss of POGZ leads to a reduced chromatin

accessibility. Regulation of chromatin under control of POGZ depends on esBAF complex. POGZ is extensively co-localized with OCT4/NANOG genome wide. Taken together, we propose that POGZ is a pluripotency-associated factor, and its absence in ESCs causes failure to maintain a proper ESC-specific chromatin state and transcriptional circuitry of pluripotency, which eventually leads to ESC self-renewal and pluripotency defects. Our work provides important insights into the role of POGZ in ESC self-renewal and pluripotency as well as regulation of transcription, which will be useful for understanding the etiology of neurodevelopmental disorders by *POGZ* mutation.

Introduction

POGZ encodes a transcription factor that contains multiple domains, including a zinc-finger cluster, an HP1- binding motif, a CENPB-DB domain, and a transposase-derived DDE domain. POGZ is thought to primarily function a transcriptional repressor as it is a reader of heterochromatin-associated mark H3K9me3 (Vermeulen et al., 2010), is associated with heterochromatin proteins (HP1s) (Nozawa et al., 2010), and inhibits transcription by an in vitro luciferase assay (Suliman-Lavie et al., 2020). Loss of function *POGZ* mutations has been frequently linked with mesodermal-derived cardiac disease, schizophrenia, microcephaly, neuroectodermal-derived intellectual disability and autism spectrum disorders (Fukai et al., 2015; Reuter et al., 2020; Stessman et al., 2016; Tan et al., 2016; White et al., 2016; Ye et al., 2015; Zhao et al., 2019). Of note, *POGZ* is one of the top recurrently mutated genes in patients with NDDs, particularly ASD and ID (De Rubeis et al., 2014; Matrumura et al., 2020; Suliman-Lavie et al., 2020; Wang et al., 2016; Zhao et al., 2019). A recent study has reported that POGZ plays an important role in hematopoiesis (Gudmundsdottir et al., 2018).

Mouse *Pogz* mRNA is abundantly expressed during early gestation and reaches its maximum expression on E9.5. *Pogz-/-* mice are embryonic lethal, and rarely survived beyond embryonic day 16.5 (E16.5) when neurogenesis takes place (Gudmundsdottir et al., 2018). These observations suggest that POGZ may play important roles in inner cell mass and embryonic stem cell maintenance, and proper formation of three germ layers, especially the neural lineage.

The SWItch/Sucrose Non-Fermentable (SWI/SNF) ATP-dependent remodelers are highly evolutionarily conserved complexes, which include the two mutually exclusive ATPase subunits SMARCA4/BRG1 and SMARCA2/BRM, and core members such as SMARCC1/BAF155, SMARCC2/BAF170 and SMARCD1/BAF60a (Alver et al., 2017). This complex is known to play key roles in proliferation and differentiation in a number of different tissues and cell types, including embryonic stem cells (ESCs) in which it called the esBAF (Ho et al., 2008; Panamarova et al., 2016). The SWI/SNF complex can regulate gene expression by displacing nucleosomes proximal to gene promoters and by modulating enhancer function (Alver et al., 2017; Ho et al., 2009). The regulation of SWI/SNF complex activity can be achieved via subunit composition and by interaction with tissue-specific transcription factors via its core subunits such as BRG1 (Narayanan et al., 2018; Ninkovic et al., 2013; Xiong et al., 2015). The role of esBAF complex in ESCs has been intensively studied. BRG1 is required for ESC self-renewal and pluripotency, by modulating chromatin accessibility at key regulatory elements (Kidder et al., 2009; King and Klose, 2019; Lei et al., 2015). Disruption of other esBAF core subunits, such as BAF60a, BAF250a and BAF155, also results in disruption of ESC self-renewal and pluripotency defects (Alajem et al., 2015; Gao et al., 2008; Gao et al., 2019; Ho et al., 2008; Liu et al., 2020; Schaniel et al., 2009; Takebayashi et al., 2013; Zhang et al., 2014).

In this work, we show that POGZ plays a key role in ESC self-renewal and pluripotency, by recruiting the esBAF/BRG1 complex and HP1 proteins. Loss of

POGZ leads to ESC differentiation towards PrE cell types, likely by up-regulation of *Gata6* and *Sox17* and by down-regulation of pluripotency-related genes. POGZ, esBAF/BRG1 and core pluripotency factors are co-localized genome-wide and extensively co-occupy enhancers, including super-enhancers. POGZ-regulated local chromatin accessibility depends on esBAF/BRG1, and they control gene expression by modulating chromatin accessibility and nucleosome occupancy. POGZ interacts with both BRG1 and HP1 proteins using its distinct domains, and they can form a triplex which we designate as PBH. POGZ recruits BRG1 and HP1 proteins to target genes in a DNA sequence specific manner. Our work suggested that POGZ is a pluripotency-associated factor that regulates gene expression by association with esBAF/BRG1 complex and HP1 proteins.

Results:

Generation and characterization of *Pogz-/-* ESCs

To understand the function of POGZ, we generated *Pogz-/-* ESCs by CRISPR/Cas9 technology. The guide RNAs (gRNAs) were designed targeting the exon 2 of the *Pogz* gene (Figure 1A). We have successfully generated at least 3 mutant alleles (1 bp deletion, 7 bp insertion, and 284 bp insertion in exon 2 of the *Pogz* gene) (Figure 1B; Supplementary Figure 1A). ESCs bearing mutant allele (-1 bp) were chosen to perform the majority of the subsequent experiments, and ESCs with other mutant alleles (+7/284 bp) were used to confirm the results when it was necessary. The qRT-PCR analysis showed that *Pogz* mRNA levels were greatly reduced in mutant

ESCs compared to controls (Figure 1C). Western blotting results showed that POGZ protein was hardly detectable in mutant ESCs using POGZ antibodies of different resources (Figure 1D), which suggested that *Pogz* mutant alleles are functional nulls.

Early passage *Pogz-/-* ESCs in the traditional self-renewal medium containing the LIF/KSR remained undifferentiated, as they displayed typical ESC-like domed morphology, and abundantly expressed pluripotency markers OCT4 and NANOG (Figure 1E). However, an obvious cell proliferation defect was observed in *Pogz-/-* ESCs as well as *Pogz+/-* ESCs (Figure 1F), which was confirmed by immunofluorescence (IF) staining of the cell division marker phospho-Histone H3 (PH3) (Supplementary Figure 1B). This observation was in line with a previous report that POGZ is essential for normal mitotic progression of cells (Nozawa 2010). It also suggested that haploinsufficiency of *Pogz* can lead to ESC proliferation defect similar to loss of *Pogz*. After 6-10 passages, however, many *Pogz-/-* ESCs adopted a flatten morphology and lacked of tight cell contacts, suggesting that they were undergoing spontaneous differentiation (Figure 1G). This was confirmed by alkaline phosphotase (AP) staining as the fattened cells exhibited reduced AP activities (Figure 1H). Consistently, there was a significantly decreased expression of pluripotency genes such as *Nanog* and *Sox2*, and a significant up-regulation of lineage determination genes, in particular the primitive endoderm (PrE) markers such as *Gata6* and *Sox17* (Figure 1I). We confirmed the aberrant up-regulation of PrE marker GATA6 and the down-regulation of OCT4 at protein levels, by IF and Western blotting, respectively (Figure 1J-K; Supplementary Figure 1C). Importantly, restoring FLAG-POGZ in

Pogz-/- ESCs rescued the expression defects of Gata6 and OCT4, demonstrating the specificity of the phenotype. Thus, our data suggested that acute depletion of POGZ does not lead to immediate loss of self-renewal, while its prolonged depletion causes ESC undergoing differentiation.

To comprehensively understand how POGZ deficiency affects ES cell phenotype, we performed RNA-seq analysis for early passage control and *Pogz-/-* ESCs. A total of 4423 differentially expressed genes (DEGs) were identified (Figure 1L). Of which, 2207 genes were up-regulated and 2216 genes down-regulated. GO analysis showed that the DEGs were enriched for terms such as regulation of nervous system development and neuronal projection, axonogenesis and muscle development (Figure 1M). KEGG analysis of DEGs revealed the enrichment of terms such as calcium signaling pathway and pathways in cardiac development and diseases (Figure 1N). Specifically, the expression of pluripotency-associated genes such as *Sox2*, *Nanog*, *Dpp3/4*, *Utf1*, *lefty2* and *Tdgf1* was decreased in mutant ESCs compared to control ESCs. Strikingly, a panel of primitive endoderm genes such as *Gata6*, *Gata4*, *Sox17*, *Sox7*, *Sparc*, *Cited, Cubn* and *Dab2*, were significantly up-regulated (fold change> 2; $P< 0.05$). Mesodermal genes such as *Gata3*, *Bmper*, *Edn1*, *Fzd10*, *Nfatc1*, *Has2*, *Irx2*, *Stat1*, *Tbx20*, *Nkx2.9*, *Nkx6.2*, *Nodal*, *Foxi3/q1* and *Wnt6/10*, were also up-regulated. By contrast, the expression of neuroectodermal progenitor genes such as *Fgf5*, *Sox1*, *Pax6* and *Nes* was largely unchanged. Interestingly, *Nefh/Nefl/Nefm* which are involved in the maintenance of neuronal caliber, was markedly up-regulated. Moreover, Hippo-YAP pathway target genes *Ctgf*, *Fat1*, *Vgll3* and *Lats2*, and

epithelial to mesenchymal transition (EMT) genes such as *Zeb1/2*, *Twist1*, *Notch2/3* and *Id2* were up-regulated.

Based on the above results, we concluded that POGZ is essential for the maintenance of ESC undifferentiated state. Loss of POGZ leads to ESC undergoing differentiation, likely by up-regulation of primitive endoderm and mesoderm lineage genes and by down-regulation of pluripotency-associated genes.

Loss of POGZ leads to compromised pluripotency

Next, we asked whether loss of POGZ leads to ESC pluripotency defects. To this end, we performed embryoid bodies (EBs) formation assay for control and early passage mutant ESCs. EBs from control ESCs were round and large, whereas *Pogz-/-* ESC-derived EBs were irregular in shape and smaller in size, suggesting that there was a defect in EB formation (Figure 2A; Supplementary Figure 2A).

To investigate this further, qRT-PCR analysis was performed to carefully examine the expression of pluripotency and early lineage-specifying genes for a time course of 8 days. Of note, the dynamic expression pattern of *Pogz* closely mimicked that of pluripotency TF genes *Pou5f1* and *Nanog,* as ESCs differentiated under EB induction condition (Figure 2B). During EB formation of control ESCs, both core pluripotency genes and *Pogz* were gradually down-regulated, while lineage-specifying genes (neuroectoderm, mesoderm and endoderm genes) were gradually induced and peaked at day 5-6. During *Pogz-/-* ESC EB formation, however, neuroectodermal genes such as *Sox1*, *Nes* and *Pax6*, and endodermal markers such as

Gata6 and *Sox17* were markedly down-regulated (fold change> 2; $P< 0.05$). By contrast, mesodermal genes such as *Tbx20*, *T* and *Gsc*, were markedly up-regulated. Thus, the time-course qRT-PCR analysis indicated that there was a pluripotency defect of *Pogz-/-* ESCs.

To comprehensively understand how ESC pluripotency was affected in the absence of POGZ, we performed RNA-seq analysis for day 6 control and mutant ESC-derived EBs. A total of 6,760 DEGs were identified when fold change was set for 1.5 ($P< 0.05$). Of which, 3,353 genes were down-regulated, and 3,407 genes were up-regulated. When the fold change was set for 2 ($P< 0.05$), a total of 2,442 DEGs were identified (Figure 2C). Of which, 1,222 genes were down-regulated, and 1,220 genes were up-regulated. GO analysis of DEGs showed that they were enriched for terms such regulation of neurotransmitter levels, axon finding, synapse and neuron projection (Figure 2D). KEGG analysis of DEGs revealed the enriched terms such as pathways in regulation of cardiac development and metabolism (Figure 2E). Specifically, mesodermal genes such as *Wnt2//6/11*, *Fzd1/2/3/6/7/8*, *Tbx2/3/20*, *Hand1/2*, *Foxf1*, *Isl1, Gata2/3/4/5, Bmper*, *Isl1*, *Nkx2.5* and *Foxa3*, were significantly up-regulated, many of which were cardiac-developmental genes. By contrast, neuroectodermal genes such as *Pax6*, *Nes*, *Sox1/10* and *Fgf5*, and pluripotency-related genes such as *Nanog*, *Sox2, Pou5f1* and *Utf1* were markedly down-regulated. Of note, the down-regulation of neuroectodermal lineage genes was in line with that mutations of *POGZ* are frequently linked with neurodevelopmental disorders such as autism syndrome disorders (ASD) (Matrumura et al., 2020; Nozawa et al., 2018). The heat

map analysis was used for the representative genes, including the pluripotency and the neural genes (Figure 2F).

Taken together, we concluded that POGZ is required to restrain the expression of lineage-specifying genes in ESCs. Under EB induction condition, *Pogz-/-* ESCs differentiate towards mesodermal cell types at the expense of neuroectodermal lineage, emphasizing the critical role of POGZ in neural induction and differentiation.

POGZ physically associates with the esBAF complex and HP1 proteins

To understand the mechanisms by which POGZ may regulate ESC self-renewal and pluripotency, we performed IP combined with mass spectrometry assay (IP-Mass Spec) to identify its potential interaction proteins. A total of 78 proteins, including the known POGZ interacting protein HP1γ/CBX3, were identified by the IP-Mass Spec compared to the IG control (Nozawa et al., 2010; Vermeulen et al., 2010). Interestingly, members of the esBAF complex and its associated factors, including SALL4, Nono, Sfpq, Mybbp1a, Actin, ACTG1, Smarcc1/BAF155 and Smarcd1/BAF60A, were highly represented (Figure 3A). BAF155, BAF60A and ACTG1 are well-known members of the SWI/SNW chromatin remodeling complex (called the esBAF in ESCs) and are involved in the regulation of ESC maintenance and differentiation (Alajem et al., 2015; Kim et al., 2001; Ho et al., 2008; 2009; Panamarova et al., 2016; Ramanathan et al., 2018; Schaniel et al., 2009). SALL4, Nono, Sfpq and Mybbp1a are previously known esBAF-associated proteins in ESCs (Ho et al., 2009). Thus, our IP-Mass Spec experiments strongly suggested that POGZ

is cellular protein which is closely-related to the esBAF complex in ESCs.

The IP-Mass Spec results were unexpected, as previous work have suggested that POGZ is involved in transcriptional repression and is tightly linked with repressive chromatin regulators such as CHD4 and HP1 proteins (Nozawa et al., 2010; Ostapcuk et al., 2018; Suliman-Lavie et al., 2020). CHD4, the core catalytic subunit of NuRD chromatin remodeling complex, has been repeatedly purified as a POGZ-related chromatin remodeler in ESCs (Ostapcuk et al., 2018; Vermeulen et al., 2010). HP1 proteins, originally identified as structural proteins of heterochromatin, are important for heterochromatin-mediated gene silencing (Mattout et al., 2015). To substantiate our finding, co-IP experiments were performed to examine whether POGZ interacts with members of the esBAF complex, as well as CHD4. HP1γ was included as a positive control, as all three isoforms of HP1 proteins have been shown to interact with POGZ in Hela cells (Nozawa et a., 2010). The co-IP results showed that POGZ was able to readily pull down HP1γ, which was further supported by double immunofluorescence staining using antibodies against POGZ and HP1γ (Supplementary Figure 3A). POGZ appeared to strongly associate with BRG1, and weakly interact with BAF155. By contrast, POGZ failed to pull down CHD4 (Figure 3B). Based on the biochemistry data, we concluded that POGZ is closely linked with the esBAF/BRG1 complex, but not the NuRD/CHD4 complex.

Next, we asked whether POGZ physically associates with the esBAF complex. To this end, we used the TnT in vitro translation system (Promega) to synthesize POGZ, FLAG-BRG1 and FLAG-BAF155. When POGZ and FLAG-BRG1 were

mixed together, POGZ readily pulled down both FLAG-BRG1. Similar results were observed for FLAG-BAF155 (Figure 3D; Supplementary Figure 3B). Furthermore, double IF staining of BRG1 and POGZ clearly showed that they were co-localized in the nuclei of ESCs (Supplementary Figure 3C). Based on these results, we concluded that POGZ directly interacts with BRG1 and BAF155 of the esBAF complex.

Because BRG1 is the core ATPase subunit of esBAF, we consider BRG1 to be the representative of the esBAF complex in our following experiments. Next, we mapped the interaction domains between POGZ with BRG1. Constructs encoding various truncated forms of POGZ and BRG1 were co-transfected into in HEK293T cells, and co-IP experiments were performed (Figure 3E). The mapping results showed that the N-terminal fragment but not the C-terminal fragment of POGZ is responsible to interact with BRG1 (Figure 3F; Supplementary Figure 3D-E). Further mapping showed that the N-terminal fragment of BRG1 (1-446 aa) mediates its interaction with POGZ-Nter (Figure 3G). Thus, POGZ interacts with BRG1 via its N-terminal fragment.

The interacting domain of POGZ (called HPZ) for HP1 proteins has been determined (Nozawa et al., 2010). As POGZ used its N-terminal fragment for association with BRG1 and its HPZ motif for HP1s, we speculated that POGZ, BRG1 and HP1 may form a tripartite complex (the PBH triplex, thereafter). To test this possibility, we performed the sequential immunoprecipitation experiments for POGZ, BRG1 and HP1γ. Here, HP1γ but not HP1α and β was selected because HP1γ is highly represented in our IP-Mass Spec and importantly, is required for proper ESC

self-renewal and pluripotency similar to POGZ and BRG1 (Mattout et al., 2015; Sridharan et al., 2013; Zaidan and Sridharan, 2020). In the first round of IP, FLAG-POGZ readily pulled down BRG1. In the second round of IP, BRG1 readily pulled down HP1γ (Figure 3H). Thus, our sequential IP results strongly suggested that POGZ, BRG1 and HP1γ can form the PBH triplex (Figure 3I), although the triplex is obviously a part of a much larger complexes containing other esBAF members such as BAF155 and BAF60A (for this, PBH also stands for POGZ, esBAF and HP1).

Genome-wide binding profile of POGZ

To further understand the function of POGZ in the maintenance of ESCs and regulation of gene expression, we performed ChIP-seq experiments using different sources of commercial POGZ antibodies. Unfortunately, the commercial antibodies, which were good in Western blotting and/or IF applications, failed to work in ChIP-seq experiments. We therefore established the FLAG-POGZ restoring *Pogz-/-* ESC lines and performed the ChIP-seq experiments using FLAG antibodies. Before performing the ChIP-seq, we confirmed that FLAG-POGZ was expressed at similar levels to control ESCs. Recently, the CUT&Tag, a newly developed enzyme-tethering technique, has been shown to be more efficient than the traditional ChIP-seq assay (Kaya-Okur et al., 2019). We therefore utilized this method in parallel.

A total of 7,929 peaks were identified, based on the FLAG ChIP-seq experiments. By contrast, a total of 16,728 peaks were revealed by the CUT&Tag. In addition to the larger number of POGZ peaks, the binding intensity by CUT&Tag was much stronger

than the traditional ChIP-seq, which suggested that CUT&Tag performed better than the FLAG ChIP-seq. The snapshots of *Dcp1a* and *Chchd1* loci were shown for representatives (Supplementary Figure 4A).

Analysis of both the CUT&Tag and FLAG ChIP-seq signals revealed that POGZ peaks were primarily localized to the proximal Transcription Start Site (TSS) and distal regions (Figure 4A-C). As CUT&Tag produced more information than the ChIP-seq, our following bioinformatics analysis was primarily based on the data from the CUT&Tag. We found that POGZ peaks at distal regions were highly overlapped with H3K4me1 and H3K27ac, known histone marks for poised and active enhancers, respectively (Supplementary Figure 4B). Thus, POGZ peaks were highly localized to proximal TSS and enhancer regions, which implied that POGZ regulates transcription by binding to key regulatory elements of its target genes.

A total of approximately 11,000 target genes were bound by POGZ. GO analysis of POGZ target genes revealed the enrichment for terms such as regulation of synaptic function, regulation of neuron apoptosis, glutamate receptor activities, astrocyte projection, and regulation of chromatin (Figure 4D). KEGG analysis of POGZ target genes showed the enrichment of terms such as phospholipase signaling pathway, Parkinson diseases, glutamatergic synapse and neuroactive ligand-receptor interaction (Figure 4E). Both GO and KEGG analyses indicated that POGZ is overwhelmingly linked with neuronal function and disorders. This was in line with that POGZ is one of the most recurrently mutated genes in patients with neurodevelopmental disorders, particularly ASD and ID (intellectual disability)

(Matrumura et al., 2020; Zhao et al., 2019).

POGZ is a typical transcription factor, suggesting that it binds to DNA in a sequence specific manner. Motif analysis of POGZ-bound sites by HOMER revealed a series of consensus DNA motifs (Supplementary Figure 4C). The top enriched DNA motif is GGGGCGGGGC (67% of peaks) with extremely high significance (Figure 4F). This motif is enriched with GC, analogous to the CpG island, which may explain why POGZ peaks were enriched at the proximal TSS (Blackledge et al., 2014). In addition, this motif is a consensus binding motif for SP1 and KLFs. KLF4 is a well-known ESC pluripotency factor. SP1, which has been shown to be a POGZ interactor in a two-hybrid screening, is involved in transcription regulation (Gunther et al., 2000). Strikingly, ATTTGCAT, the putative binding motif of ESC core pluripotency factors (Boyer et al., 2005; Loh et al., 2006), was enriched with high significance (Figure 4F). It is well-known that core pluripotency factors such as OCT4 and SOX2 co-occupy both ESC-specific genes and lineage-specifying genes by binding to this motif, promoting the former and repressing the latter (Boyer et al., 2005). When a few pluripotency and lineage-specifying genes were examined, POGZ indeed exhibited enrichment at these genes, similar to the core pluripotency factors (Figure 4G). However, POGZ did not bind to the key mesodermal marker genes *Gsc* and *T*. The snapshots were shown for representative genes, including neural progenitor genes such as *Pax6*, *Nes*, *Sox1* and *Olig2*, endodermal regulatory genes such as *Gata6* and *Sox17*, mesodermal genes such as *T* and *Gsc*, and pluripotency TF genes such as *Pou5f1* and *Nanog* (Figure 4G; Supplementary Figure 4B).

As POGZ binds DNA motifs that are also bound by the core pluripotency factors OCT4/KLF4, we asked whether POGZ is co-localized with NANOG/OCT4 genome wide. To this end, we consulted the published NANOG/OCT4 ChIP-seq data sets (King and Klose, 2017). We found that there was an extensively overlap of POGZ and NANOG/OCT4 peaks genome-wide (Figure 4G-H). Approximately 6,560 peaks (about 64% of all NANOG peaks) were shared between POGZ and NANOG, and 5,414 sites (about 73% of all OCT4 peaks) were shared between POGZ and OCT4 (Figure 4I). Furthermore, at distal and genic regions of some pluripotency-related and developmental genes, broad POGZ CUT&Tag signals (around 5 kb) were observed (Figure 4G; Supplementary Figure 4B). This feature of binding was analogous to the previously described super-enhancers (Pott and Lieb, 2014). The super-enhancers are a recent identified enhancer type that marked by a high levels of Mediator and P300/H3K27Ac (Whyte et al., 2013). We speculate that POGZ may bind to super-enhancers, similar to OCT4/NANOG. When examining the ChIP-seq signals for POGZ, NANOG, OCT4, MED1, H3K4me1 and H3K27ac, we found that POGZ co-occupied with these super-enhancer-related marks, confirming that POGZ binds super-enhancers (Figure 4J). Thus, super-enhancers in ESCs are bound and likely regulated by POGZ.

The above co-localization analysis of POGZ and OCT4/NANOG revealed very high degrees of target gene overlap (Figure 4H-I). This strongly suggested that POGZ may functionally interact with the core pluripotency factors at the target genes. We therefore asked whether POGZ and OCT4 interact with each other in ESCs. In

support of this notion, double IF staining showed that POGZ and OCT4 were co-localized in the nuclei of ESCs (Figure 4K). The co-IP experiments showed that POGZ could readily pull down endogenous OCT4 (Figure 4L).

Taken together, we concluded that POGZ is extensively co-localized with core pluripotency factors genome-wide, and interacts with core pluripotency factors in ESCs. This raised an interesting possibility that POGZ is an important pluripotency-associated factor.

POGZ, BRG1 and HP1 are extensively co-localized genome-wide

As POGZ associates with esBAF and HP1 proteins in ESCs, we asked whether the three factors were co-localized genome wide. We consulted the previously published ChIP-seq data for BRG1 and HP1 proteins (King and Klose, 2018; Sridharan et al., 2013). A total of 12,414 BRG1 binding sites were identified. BRG1 ChIP-seq peaks were localized to enhancer and proximal TSS regions, as previously reported (Kidder et al., 2009; Ho et al., 2008; Ostapcuk et al., 2018). A total of 6,570 HP1γ binding sites were identified. HP1γ ChIP-seq peaks were localized to TSS and sites nearby the Transcription End Site (TES), as recently described (Zaidan and Sridharan, 2020).

Analysis of ChIP-seq data sets showed that POGZ, BRG1 and HP1 proteins are extensively co-localized genome-wide (Figure 5A; Supplementary Figure 5A). POGZ and BRG1 co-occupied with HP1γ and HP1β at both the POGZ peak center and the proximal TSS regions (Figure 5B). Approximately 73% (8165/1240) of POGZ peaks were overlapped with 66% (8165/12415) of BRG1 peaks. About 71%

(4654/6570) of HP1γ peaks were overlapped with 41% (4654/11240) of POGZ peaks. About 70% (4607/6570) HP1γ peaks were overlapped with 37% of BRG1 peaks. When examining the sites bound by all three factors, approximately 3,691 peaks were identified, representing 56% of all HP1γ peaks (Figure 5C). GO analysis of the shared genes (by all three factors) showed the enrichment of terms such as regulation of cell cycle, chromatin modification and regulation of transcription (Figure 5D; up). KEGG analysis of the shared genes revealed the enrichment of the Hippo signaling pathway, cell cycle and germ cell formation (Figure 5D; bottom).

To gain insights into the relationship between PBH binding and gene expression regulation, we plotted POGZ CUT&Tag, BRG1 and HP1γ ChIP-seq reads in a ± 3 kb region surrounding the TSS and divided POGZ-, HP1γ- and BRG1-bound genes into 7 categories (cluster A: $POGZ^{+}BRG1^{+}HP1^{+}$; cluster B: $POGZ^{+}BRG1^{-}HP1^{+}$, cluster C: $POGZ^{+}BRG1^{+}HP1^{-}$, cluster D: $POGZ^{+}BRG1^{-}$HP1-, cluster E: $POGZ^{-}BRG1^{+}HP1^{+}$, cluster F: $POGZ^{-}BRG1^{-}HP1^{+}$, cluster G: $POGZ^{-}BRG1^{+}HP1^{-}$) (Figure 5E). We found that compared to all genes, the average mRNA expression levels of clusters A/B (PBH- and PH-bound genes) are much higher than the other clusters (Figure 5F). In fact, both HP1γ and BRG1 ChIP-seq peaks have been shown to be enriched surrounding the proximal TSS, and importantly, their enrichment levels are positively correlated with gene expression levels: namely, the higher the gene expression levels, the more enrichment of HP1γ and BRG1 at TSS (Ho et al., 2009; Zaidan and Sridharan, 2020). Therefore, the above division of 7 gene clusters was actually rather arbitrary. Instead, actively-transcribed pluripotency TF genes such as

Pou5f1/Nanog/Sox2 in cluster A should be designated as $POGZ^{+}BRG1^{high}HP1^{high}$, and lowly-expressed developmental genes such as *Gata6/Sox17* should belong to cluster C ($POGZ^{+}BRG1^{low}HP1^{low}$), and *T* and *Gsc* should belong to $POGZ^{-}BRG1^{low}HP1^{low}$. Snapshots of the representative genes were shown (Supplementary Figure 5B).

Next, we analyzed the effects of loss of POGZ on the expression of each cluster of genes (Figure 5G). The results showed that loss of POGZ leads to a slight but significant down-regulation of genes in clusters A, B and F, but had little effects on expression of other clusters. These observations suggested that HP1γ-bound target genes are most sensitive to loss of POGZ, and are positively regulated by POGZ.

The co-localization of PBH strongly suggested that POGZ facilitates target gene expression by recruiting HP1γ and/or BRG1. We therefore performed ChIP experiments to examine the binding of HP1γ and/or BRG1 at promoter regions of PBH-bound genes, including core pluripotency TF genes such as *Nanog* and *Pou5f1*, endodermal developmental genes such as *Gata6* and *So17*, neuroectodermal genes *Nes* and *Wnt3*, and component genes belong to Wnt and Hippo signaling pathways, in the presence and absence of POGZ. Mesodermal genes *Gsc* and *T*, although not bound by POGZ, were also included as controls (Supplementary Figure 4B). The ChIP results showed that BRG1 and HP1γ levels at the majority of examined genes except *Gsc* and *T* were markedly reduced, in the absence of POGZ (Figure 5H; Supplementary Figure 5C), despite that HP1γ levels were low at TSS regions of lowly-expressed developmental genes such as *Gata6* and *Sox17*.

We have shown that POGZ-bound genes at proximal TSS and enhancer regions

were also bound by core pluripotency factors NANOG and OCT4 (Figure 4G; 4J). A Pearson correlation analysis of ChIP-seq signals revealed a high degree of co-localization of POGZ, BRG1, HP1, NANOG and OCT4 (Figure 5I). This prompted us to ask whether the PB- or PBH-bound genes also bound by NANOG and OCT4. When we looked at a few ESC-specific and lineage specifying genes (especially neural developmental genes), core pluripotency and PBH factors were highly enriched and very well co-localized at proximal TSS and distal enhancers (Figure 5J). When we extended this to genome, we found that POGZ, BRG1, HP1γ and OCT4/NANOG were extensively co-localized genome wide (Supplementary Figure 5D). In fact, approximately 1,410 gene were bound by all these 5 factors. Thus, POGZ, BRG1, HP1γ, OCT4 and NANOG co-occupy target genes genome wide.

So far, our results strongly suggested that PBH and OCT4/NANOG work together to regulate ESC self-renewal and differentiation potential. We speculated that the PBH may support ESC self-renewal and pluripotency by controlling a cohort of similar genes or pathways. If this was the case, loss of either factor should lead to similar change in gene expression. To test this hypothesis, we consulted the previously published RNA-seq data for ESCs that are depleted of all three isoforms of HP1 and BRG1 (Hainer et al., 2015; King and Klose, 2017; Ostapcuk et al., 2018). Bioinformatics analysis revealed a considerable similarity in gene expression change among POGZ-, HP1- and BRG1-depleted ESCs. For instance, under fold change > 2 and P-value< 0.05, a total of 402 up-regulated genes and 558 down-regulated genes were shared by POGZ and HP1s (Figure 5K). When we examined the up- and

down-regulated genes shared by all three factors, the numbers were 87 and 173, respectively (Supplementary Figure 5E). Specifically, POGZ-, HP1- and BRG1-depleted ESCs all exhibited a significant up-regulation of PrE genes such as *Gata4*, *Gata6*, *Sox7* and *Sox17*, mesodermal genes such as *Edn1*, *Nfatc1* and *Stat1* as well as neural genes such as *Nefl* and *Nefm*, and a significant down-regulation of pluripotency genes such as *Nanog*, *Pou5f1* and *Sox2*. This observation strongly supported that the PBH triplex is essential for maintaining ESC pluripotency by promoting pluripotency genes and by repressing lineage-specifying genes, especially the PrE genes. In ESCs, BRG1 and core pluripotency factors are known to have dual roles in the ESC circuitry: bind the developmental genes to repress their expression, and occupy ESC-specific genes to support ESC pluripotency (Ho et al., 2009; King and Klose, 2017). Thus, similar to core pluripotency factors and BRG1, POGZ is enriched at highly expressed ESC-specific genes that are down-regulated, and at lowly expressed lineage-specifying genes that are up-regulated during ESC differentiation under EB induction condition. These observations strongly supported that POGZ is a pluripotency-associated factor.

BRG1 is the core enzymatic components of the esBAF, which included many other factors such as BAF155, BAF60a, BAF250a and SS18. The co-localization of BRG1 and POGZ prompted us to further investigate whether POGZ is co-localized with other members of the esBAF complex. To this end, we consulted the ChIP-seq data of SS18 and BAF250a/*Arid1a* (King and Klose, 2017). Examination of ChIP-seq peaks showed that POGZ, BRG1, BAF250 and SS18 were nicely co-localized

genome wide (Supplementary Figure 5F). Thus, we propose that POGZ co-localizes and recruits esBAF genome wide in ESCs.

Finally, we examined the overlap of POGZ ChIP-seq peaks with polycomb repressive proteins and its catalyzed repressive histone marks, such as EZH2/H3K27me3 and Ring1b/H2Aub1. Besides at proximal TSS regions, POGZ is extensively co-localized with enhancer marks H3K4me1/H3K27Ac but not with H3K27me3/H2Aub1 (Supplementary Figure 5G). These observations showed that POGZ occupies poised and active enhancers in ESCs, which further supported that POGZ is a pluripotency-associated factor that regulates gene expression by modulating enhancer function via esBAF. We also examined the PBH-bound sites with H3K9me3, a HP1 binding repressive histone mark in pluripotency and differentiated cells. We found that the PBH-bound sites were not enriched with H3K9me3 (data not shown).

Taken together, we propose that POGZ play important roles in ESC self-renewal and pluripotency by directly recruiting esBAF and HP1s to both ESC-specific and lineage-specifying genes, and that association with HP1s and esBAF is functional important for POGZ.

Nucleosome occupancy and positioning are altered in the absence of POGZ

The esBAF/BRG1 are well known chromatin remodeler complex that regulate chromatin accessibility. It has been recently shown that OCT4 requires BRG1 to establish an ESC-specific chromatin accessibility that is important for the

maintenance of ESC self-renewal and pluripotency (King and Klose, 2017). Considering the close-relationship between POGZ, OCT4 and BRG1/esBAF, we asked whether loss of POGZ leads to alteration of chromatin accessibility, by performing ATAC-seq analysis for control and *Pogz-/-* ESCs.

A total of approximately 10,250 ATAC-seq peaks were identified in control ESCs. The majority of POGZ-bound loci were of ATAC-seq signals, suggesting that POGZ is bound to accessible chromatin or POGZ binding renders chromatin accessible. By contrast, approximately 8,630 peaks were found in *Pogz-/-* ESCs. Thus, a total of 1,630 ATAC-seq peaks were lost in the absence of POGZ, which suggested that POGZ facilitates an accessible chromatin. Globally, the chromatin accessibility was moderately reduced in the absence of POGZ (Figure 6A-B). Bioinformatics analysis of POGZ-dependent ATAC-seq loci that exhibited change in the absence of POGZ revealed that the top three motifs are the putative DNA motifs bound by pluripotency factors OCT4 and KLF4 (Supplementary Figure 6A). Specifically, we found that the chromatin accessibility was reduced at both POGZ-bound pluripotency genes and developmental genes in the absence of POGZ (Figure 6C). The snapshots were shown for pluripotency-related genes such as *Pou5f1* and *Utf1*, endodermal genes such as *Sox7* and *Sox17*, and neuroectodermal genes such as *Pax6* and *Sox1* (Figure 6C; Supplementary Figure 6B).

Next, we asked whether BRG1 is required for POGZ-regulated accessible chromatin by examining the overlap of BRG1 ChIP-seq peaks and POGZ-dependent ATAC peaks. We found that BRG1 was highly enriched at sites where POGZ is

responsible for chromatin accessibility (Figure 6B-D). This observation suggested that POGZ may require BRG1 to shape chromatin accessibility of POGZ-bound sites and gene regulation in the maintenance of ESC state. We consulted the published ATAC-seq data for BRG1 (King and Klose, 2017). When we examined ATAC-seq signal at a few POGZ target sites in BRG1 knockout ESCs, we found a substantial reduction of chromatin accessibility, which was similar to loss of POGZ (Supplementary Figure 6C). When we examined all ATAC sites, we did observe a reduction of ATAC-seq signals for both POGZ- and BRG1-depleted ESCs compared to control ESCs, although it looked subtle (Supplementary Figure 6D). However, when we examined only POGZ-dependent ATAC sites (bound by POGZ and altered in the absence of POGZ), ATAC-seq signals at the these sites were apparently reduced in *Brg1-/-* ESCs compared to control ESCs (Figure 6E). Importantly, loss of BRG1 had a similar effect on chromatin accessibility to that by loss of POGZ, suggesting that POGZ required BRG1 to create accessible chromatin at POGZ-bound sites in ESCs.

Next, we asked whether POGZ regulates nucleosome occupancy at target genes. We found that at a global level, loss of POGZ at POGZ binding sites led to an increase of nucleosome occupancy (Figure 6F). When we examined a few pluripotency and lineage-specifying genes, we observed change of nucleosome occupancy and phasing for most of the genes (Figure 6G).

If POGZ function as a pluripotency-associated factor, loss of POGZ should lead to a similar change of chromatin accessibility to loss of BRG and OCT4. To this end,

we downloaded the published ATAC-seq data for OCT4 (King and Klose, 2017). We found that loss of POGZ, OCT4 and BRG1 leads to a similar reduction of chromatin accessibility at PBH-bound genes such as *Utf1* and *Ppp3ca* (Supplementary Figure 6C).

Finally, we went on to understand whether the alteration of chromatin accessibility is relevant to gene regulation by loss of POGZ. Globally, the expression of genes which exhibited altered ATAC-seq signals at POGZ-bound sites in the absence of POGZ was decreased in *Pogz-/-* ESCs compared to controls (Figure 6H), which suggested that POGZ is primarily required to establish an accessible chromatin and promote transcription expression. This was also in line with that the majority of DEGs were down-regulated in the absence of POGZ in ESCs (Figure 5G, K; Supplementary Figure 5E). However, we found that many genes, which exhibited significant alteration of chromatin accessibility in the absence of POGZ, were not deregulated. It appeared that alteration of chromatin accessibility of POGZ-bound genes did not always lead to gene expression alteration. This was also observed in *Pou5f1-/-* and *Adnp-/-* depleted ESCs where much more dramatic change in chromatin accessibility was observed (King and Klose, 2017; Ostapcuk et al., 2018; Sun et al., 2020).

Discussion

In this work, we show that POGZ plays a key role in ESC self-renewal and pluripotency as well as transcriptional regulation by association with the esBAF

chromatin remodeler complex and heterochromatin protein 1 (HP1) proteins. POGZ is essential for the maintenance of ESC undifferentiated state, and loss of POGZ leads to ESC differentiation, likely by up-regulation of primitive endoderm and mesoderm lineage genes and by down-regulation of pluripotency-related genes. Using ESC EB formation as a model, we show that POGZ is required to restrain the expression of lineage-specifying genes. In the absence of POGZ, the neuroectodermal genes were markedly down-regulated, while mesodermal and cardiac-related genes were significantly up-regulated. Mechanistically, POGZ may control ESC-specific gene expression by association with chromatin remodeler complex esBAF and HP1s, and they can form a PBH triplex. POGZ functions primarily to maintain an open chromatin, as loss of POGZ leads to a reduced chromatin accessibility. Regulation of chromatin under control of POGZ depends on esBAF complex. POGZ is extensively co-localized with OCT4/NANOG genome wide. Taken together, we propose that POGZ is a pluripotency-associated factor, and its absence in ESCs causes failure to maintain a proper ESC-specific chromatin state and transcriptional circuitry of pluripotency, which eventually leads to ESC self-renewal and pluripotency defects.

Our findings were surprising at first glance as POGZ has been shown to interact with HP1s, which reads the repressive H3K9me3 histone mark that are known associated with transcriptional repression (Vermeulen et al., 2010). POGZ was also shown to function as a negative regulator of transcription based on an in vitro GAL4-DBD luciferase assay (Suliman-Lavie et al., 2020). In addition, POGZ is frequently linked with factors such as ADNP, MGA and CHD4 which are known

transcriptional repressors (Ostapcuk et al., 2018). In this work, using biochemistry, bioinformatics and functional analyses, we found that POGZ is closely linked with esBAF complex, and POGZ can function as both a transcriptional activator and repressor, similar to the core pluripotency factors such as OCT4 and esBAF complex subunit BRG1: facilitating ESC-specific genes and suppressing lineage-specifying genes. Consistently, prolonged loss of POGZ leads to a significant down-regulation of *Nanog* and *Pou5f*1, and up-regulation of differentiation markers such as *Sox17* and *Gata6*, which eventually drives ESC loss of undifferentiated state.

POGZ is one of the top recurrently mutated genes in patients with NDDs, particularly ASD and ID. In addition to neurodevelopmental defects, *POGZ* patients may exhibit additional deficits, such as short stature, cardiac problem, hypotonia, strabismus, variable hearing loss, and abnormal craniofacial formation, including brachycephaly, long and flat malar region, broad nasal tip, short philtrum and thin vermillion border (White et al., 2016). The molecular and cellular mechanisms underlying the pleiotropic phenotypes by *POGZ* mutation remains unclear. Our work using ESC model leads to several important observations. First, POGZ might be a master regulator of neural development and neuronal function. GO analysis of POGZ target genes revealed the enrichment for terms such as regulation of synaptic function, regulation of neuron apoptosis, glutamate receptor activities and astrocyte projection. KEGG analysis of POGZ target genes showed the enrichment of terms such as Parkinson diseases, glutamatergic synapse and neuroactive ligand-receptor interaction. Both GO and KEGG analyses indicated that POGZ is overwhelmingly linked with

neuronal function and neurodevelopmental disorders. This was in line with that POGZ is one of the most recurrently mutated genes in patients with neurodevelopmental disorders. Second, POGZ associates and recruits esBAF and HP1s genome wide. It is known that esBAF complex and HP1s can control many downstream target genes by modulating the chromatin and epigenome. Thus, it is expected that in the absence of POGZ, pluripotency-, neuroectodermal-, endodermal- and mesodermal genes were all deregulated. Furthermore, component genes of key signaling pathways (Hippo, Wnt and Bmp) were also de-regulated. Third, POGZ is a pluripotency-associated factor. POGZ interacts with OCT4, and there is an extensive overlap of POGZ and NANOG/OCT4 peaks genome-wide. Approximately 64% of all NANOG peaks were shared by POGZ, and even 73% of all OCT4 peaks were shared by POGZ. POGZ binding motifs are exactly the ones bound by OCT4 and KLF4. Loss of POGZ leads to reduction of OCT4 at both mRNA levels and protein levels, which could be reversed by restoring FLAG-POGZ. In addition, loss of POGZ leads to a similar chromatin change to loss of OCT4. In fact, POGZ-associated BRG1 and HP1s are known pluripotency-associated factors (King and Klose, 2017; Mattout et al., 2015; Zaidan and Sridharan, 2020). Taken together, it can be concluded that POGZ is a multifunctional protein that is involved in the regulation of core pluripotency network, gene expression, chromatin remodeling, signaling pathways, genome architecture and epigenome. Dysfunction in any of these processes can lead to developmental defects as shown in animal models. These findings may explain the pleiotropic phenotypes observed in *POGZ* patients.

Recently, another high ASD risk factor, ADNP, has been shown to interact with chromatin remodeler CHD4 and HP1s and they form a triplex known as the ChAHP in ESCs. ADNP and POGZ belong to C2H2 type zinc finger of transcription factors, and both are the most recurrently mutated genes in ASD (Sun et al., 2020). Each factor can form a triplex with chromatin remodeler complex and HP1s, which was very interesting. We propose that HP1s and chromatin remodelers such as BRG1 and CHD4 may act as co-factors for the two DNA-binding TFs to control target gene expression.

How the different chromatin remodeler complexes and HP1s are localized to specific genome loci is an important yet unsolved question. ADNP has been shown to recruit CHD4 to the target sites in a DNA sequence specific manner (Ostapcuk et al., 2018). In this work, we show that POGZ recruits BRG1 to POGZ-bound sites in a similar way. Although lack of a global ChIP-seq analysis, our ChIP-PCR analysis using BRG1 antibodies showed that loss of POGZ leads to almost complete loss of BRG1 at a panel of genes that we examined, which strongly suggested that POGZ recruits BRG1 (therefore esBAF) to the target sites. Work by us and others suggest that DNA-binding TFs, particularly the C2H2-type zinc finger of transcription factors, are likely important players.

Methods

ES Cell Culture. Mouse embryonic stem cells (mESCs) R1 were maintained in Dulbecco's Modified Eagle Medium (DMEM, BI, 01-052-1ACS) high glucose media

containing 10% fetal bovine serum (FBS, Gibco, 10099141), 10% knockout serum replacement (KSR, Gibco, 10828028), 1 mM sodium pyruvate (Sigma, S8636), 2 mM L-Glutamine (Sigma, G7513), 1,000 U/ml leukemia inhibitory factor (LIF, Millipore, ESG1107,) and penicillin/streptomycin (Gibco, 15140-122) at 37°C with 5% CO2.

Embryoid body formation. ESCs differentiation into embryoid bodies (EBs) was performed in attachment or suspension culture in medium lacking LIF or knockout serum replacement (KSR), as described previously (Sun et al., 2020).

Generation of *Pogz-/-* ESCs. *Pogz-/-* mESCs were generated by CRISPR/Cas9 technology (Ran et al., 2013). Briefly, we designed two gRNAs on exon 2 of *Pogz* gene by using the online website http://crispr.mit.edu/. The gRNAs sequences are 5'-CGACCTGTTTATGGAATGTGAGG-3'. gRNAs were cloned into the pUC57-U6 expression vector with G418 resistance. After 48 hours of targeting plasmids transfection, mESCs were selected with 500 μg/ml G418 for 7 days. Then the cells were re-seeded on a 10-cm dish coated with 0.1% gelatin to form colonies. The single colony was picked up, trypsinized and passaged at low density. DNA from single colonies from the passaged cells was extracted and used for genotyping.

Generation of 3×Flag Tagged POGZ *Pogz-/-* mESC Cell Lines. The full-length *Pogz* cDNA (NM_172683.4) was amplified by PCR and then cloned into pCMV-3×Flag vector. The full-length *Pogz* cDNA sequence containing N-terminal 3×Flag sequence was subcloned into pCAG-IRES-Puro vector. To make stable transgenic cells, *Pogz-/-* mESCs were transfected with pCAG-IRES-Puro-3×FLAG-*Pogz* vector using Lipofectamine 2000 (Gibco,

11668019). 48 hours later, cells were selected by 1 μg/ml puromycin. After 4-5 days drug selection, cells were expanded and passaged. Western Blot assay was performed to confirm the transgenic cell line using FLAG antibodies.

RNA preparation, RT-qPCR and RNA-seq. Total RNA from mESCs and ESC-derived EBs was extracted with a Total RNA kit (Omega, R6834-01). A total of 1 μg RNA was reverse transcribed into cDNA using the TransScript All-in-One First-Strand cDNA synthesis Supermix (Transgen Biotech, China, AT341). Quantitative real-time PCR (qRT-PCR) was performed using the TransStart® Tip Green qPCR SuperMix (Transgen Biotech, China, AQ-141). The primers used for qRT-PCR were previously described (Sun et al. 2020). All experiments were repeated for at least three times. The relative gene expression levels were calculated based on the $2^{-\Delta\Delta Ct}$ method. Data were shown as means ± S.D. The Student's t test was used for the statistical analysis. The significance is indicated as follows: *, $p < 0.05$; **, $p < 0.01$; ***, $p < 0.001$.

For RNA-seq, control and mutant ESCs, and day 6 control and *Pogz-/-* ESC-derived EBs were collected and treated with Trizol (Invitrogen). RNAs were quantified by a Nanodrop instrument, and sent to BGI Shenzhen (Wuhan, China) for making RNA-seq libraries and deep sequencing. For each time points, at least two biological repeats were sequenced. DEGs were defined by FDR < 0.05 and a Log2 fold change > 1 fold was deemed to be differentially expressed genes (DEGs). Less strictly, genes whose expression differed by > 1.5 with a p-value < 0.05 were deemed differentially expresssed genes (DEGs).

We consulted RNA-seq for HP1 KO ESCs (GSM2582351-2582353; GSM2582375), for *Brg1-/-* ESCs (GSM2341328-2341333; GSM734277-79) (King and Klose, 2017; Ostapcuk et al., 2018; Sridharan et al., 2013).

Protein extraction and Western blot analysis. For protein extraction, ESCs or HEK293T cells were harvested and lysed in TEN buffer (50 mM Tris-HCl, 150 mM NaCl, 5 mM EDTA, 1% Triton X-100, 0.5% Na-Deoxycholate, supplement with Roche cOmplete Protease Inhibitor). The lysates were quantified by the Bradford method and equal amount of proteins were loaded for Western blot assay. Antibodies used for WB were POGZ (Abcam, ab171934), anti-BRG1 (Proteintech, 21634-1-AP), anti-HP1gamma (Proteintech, 11650-2-AP), anti-CHD4 (Proteintech, 14173-1-AP), anti-OCT4 (Proteintech, 60242-1-Ig), Anti-FLAG (F1804/F3165, Sigma, 1: 1000), anti-MYC antibody (Transgen Biotech, HT101) and anti-HA (Abbkine, A02040, 1: 1000). Briefly, the proteins were separated by 10% SDS-PAGE and transferred to a PVDF membrane. After blocking with 5% (w/v) non-fat milk for 1 hour at room temperature, the membrane was incubated overnight at 4ºC with the primary antibodies. Then the membranes were incubated with a HRP-conjugated goat anti-rabbit IgG (GtxRb-003-DHRPX, ImmunoReagents, 1: 5000), a HRP-linked anti-mouse IgG (7076S, Cell Signaling Technology, 1: 5000) for 1 hour at room temperature. The GE ImageQuant LAS4000 mini luminescent image analyzer was used for photographing. Western blot experiments were repeated at least two times.

Quantification of Western blot bands was performed by ImageJ software, according to the website: https://imagej.nih.gov/ij/docs/guide/146-30.html. Briefly,

the rectangle tool was selected and used to draw a box around the lane, making sure to include some of the empty gel between lanes and white space outside of the band. All lanes were selected one by one. Once all lanes are defined, go to Plot lanes to generate histograms of each lane. Then the relative values were calculated by dividing each value by the control lane. The value of the control bands was set at 1.

Co-immunoprecipitation assay (co-IP). Co-IPs were performed with the Dynabeads Protein G (Life Technologies, 10004D) according to the manufacturer's instructions. Briefly, 1.5 mg Dynabeads was conjugated with antibodies or IgG overnight at 4ºC. Antibodies were used are: 10 μg IgG (Proteintech, B900610), or 10 μg anti-POGZ antibody, or 10 μg anti-FLAG antibody (Sigma, F3165/F1804), or 10 μg anti-HA antibody (Abbkine, A02040) or 10 μg anti-MYC antibody (Transgen Biotech, HT101). The next day, total cell lysates and the antibody-conjugated Dynabeads were incubated overnight at 4ºC with shaking. After three-times washing with PBS containing 0.1% Tween, the beads were boiled at 95ºC for 5 minutes with the 6×Protein loading buffer and the supernatant was collected for future WB analysis.

Immunofluorescence assay. ESCs or EBs were collected and fixed with 4% paraformaldehyde for half an hour at room temperature. Then the cells were washed with PBST (phosphate-buffered saline, 0.1% Triton X-100) for three times, each for 15 minutes. Following the incubation with blocking buffer (5% normal horse serum, 0.1% Triton X-100, in PBS) for 2 hours at room temperature, the cells were incubated with primary antibodies at 4ºC overnight. After three-times wash with PBST, the cells were incubated with secondary antibodies (1: 500 dilution in blocking buffer, Alexa

Fluor 488, Life Technologies) at room temperature for 1 hour in the dark. The nuclei were counter-stained with DAPI (Sigma, D9542, 1: 1000). After washing with PBS for twice, the slides were mounted with 100% glycerol on histological slides. Images were taken by a Leica SP8 laser scanning confocal microscope (Wetzlar, Germany). About 10 images were taken for each slide at different magnifications.

Immunoprecipitation in combination with mass spectrometry. For Mass Spectrometry, the IP samples (immunoprecipitated by IgG or POGZ antibody) were run on SDS-PAGE gels and stained with the Coomassie Blue. Then the entire lanes for each IP samples were cut off and transferred into a 15 ml tube containing deionized water. The treatment of the samples and the Mass Spectrometry analysis were done by GeneCreate Biological Engineering Company (Wuhan, China).

Protein-protein interaction assay using a rabbit reticulocyte lysate system. Protein-protein interaction assay using a rabbit reticulocyte lysate system has been described previously (Sun et al., 2020). Tagged-POGZ, Tagged-POGZ mutants, Tagged-BRG1 and Tagged-BRG1 mutants, and Tagged-BAF15 were synthesized using the TNT coupled reticulocyte lysate system according to the manual (Promega, L5020, USA). Briefly, 1 μg of circular PCS2- version of plasmids were added directly to the TNT lysates and incubated for 1.5 hours at 30ºC. 1 μl of the reaction products were subjected to WB assay to evaluate the synthesized protein.

For protein-protein interaction assay, 5-10 μl of the synthesized HA or FLAG tagged proteins were mixed in a 1.5 ml tube loaded with the 300 μl TEN buffer, and

the mixture was shaken for 30 minutes at room temperature. Next, IP or pull-down assay was performed using Dynabeads protein G coupled with anti-FLAG or anti-HA antibodies as described above.

Quantification and statistical analysis. Data are presented as mean values ±SD unless otherwise stated. Data were analyzed using Student's t-test analysis. Error bars represent s.e.m. Differences in means were statistically significant when $p< 0.05$. Significant levels are: *$p< 0.05$; **$P< 0.01$, and ***$P< 0.001$.

Bioinformatics

ChIP-seq analysis. ChIP-seq data were aligned in Bowtie2 (version 2.2.5) with default settings. Non-aligning and multiple mappers were filtered out. Peaks were called on replicates using the corresponding inputs as background. MACS2 (version 2.1.1) was run with the default parameters. Peaks detected in at least two out of three replicates were kept for further analysis. BigWig files displaying the full length for uniquely mapping reads were generated using the bedGraphToBigWig (UCSC binary utilities).

To investigate the co-occupancy of POGZ, BRG1 and HP1γ/CBX3, we consulted previously published ChIP-seq data sets for BRG1 (GSE87820) and HP1γ/CBX3 (GSM1081158) (Ostapcuk et al., 2018; King and Klose, 2017; Sridharan et al., 2013). To investigate the co-occupancy of POGZ with H3K4me1 and H3K27ac, we consulted previously published ChIP-seq data sets for H3K4me1 (GSM2575694) and H3K27Ac (GSM2575695) (Dieuleveult et al., 2016). OCT4 (GSM2341284),

NANOG (GSM2521520), MED1 (GSM4060038), SS18 (GSM2521508), BAF250a (GSM3318684), H3K27me3 (GSM4303791), H2Aub1 (GSM2865672) ChIP-seq data were also downloaded for this work.

ATAC-seq Analysis. Paired-end reads were aligned using Bowtie2 using default parameters. Only uniquely mapping reads were kept for further analysis. These uniquely mapping reads were used to generate bigwig genome coverage files similar to ChIP–seq. Heat maps were generated using deeptools2. For the meta-profiles, the average fragment count per 10-bp bin was normalized to the mean fragment count in the first and last five bins, which ensures that the background signal is set to one for all experiments. Merged ATAC-seq datasets were used to extract signal corresponding to nucleosome occupancy information with NucleoATAC.

For comparison analysis of POGZ, OCT4 and BRG1 ATAC-seq signals, we consulted previously published ATAC-seq data sets from Brg1 KD ESCs (GSM1941485-6), Brg1 KO ESCs (GSM2341280) and OCT4 KO ESCs (GSE87819) (Dieuleveult et al., 2016; King and Klose, 2017).

Differential Binding And Gene Expression Analysis

Significant changes in ATAC-seq were identified using the DiffBind package, a FDR < 0.05 and log2 fold change> 1 was deemed to be a significant change. Gene ontology (GO) analysis for differentially regulated genes, and heat maps were generated from averaged replicates using the command line version of deepTools2. Peak centers were calculated based on the peak regions identified by MACS (see above).

Data availability

All RNA-seq, ATAC-seq, ChIP-seq and CUT&Tag data have been deposited in the public database at Beijing Genomic Institute (BGI) at https://bigd.big.ac.cn/, with the accession number of CRA003852.

References:

Alajem et al., Differential Association of Chromatin Proteins Identifiifies BAF60a/SMARCD1 as a Regulator of Embryonic Stem Cell Differentiation. Cell Reports, 10: 2019–2031 (2015)

Alver et al. The SWI/SNF chromatin remodelling complex is required for maintenance of lineage specific enhancers. NATURE COMMUNICATIONS, 8:14648 | DOI: 10.1038/ncomms14648 (2017)

Boyer et al., Core Transcriptional Regulatory Circuitry in Human Embryonic Stem Cells. Cell, 205, Vol. 122, 947 – 956 (2006)

Caillier et al.. Role of the epigenetic regulator HP1gamma in the control of embryonic stem cell properties. PLoS One. 2010; 5:e15507.

Cunniff et al. Altered hippocampal-prefrontal communication during anxiety-related avoidance in mice deficient for the autism associated gene Pogz. eLife, 9:e54835. DOI: https://doi.org/10.7554/eLife.54835 (2020)

De Rubeis et al. Synaptic, transcriptional and chromatin genes disrupted in autism. Nature 515, 209 – 215 (2014).

Dieuleveult, M., Yen, K. Y., Hmitou, I., Depaux, A., Boussouar, F., Dargham, D. B., et al.. Genome-wide nucleosome specificity and function of chromatin remodellers in

ES cells. Nature 530, 113–116. doi: 10.1038/nature16505 (2016)

Fukai, R. et al. A case of autism spectrum disorder arising from a de novo missense mutation in POGZ. J. Hum. Genet. 60, 277–279 (2015).

Gao et al. Heterozygous Mutations in SMARCA2 Reprogram the Enhancer Landscape by Global Retargeting of SMARCA4. Molecular Cell, 75, 891–904 (2019)

Gao, X. L., Tate, P., Hu, P., Tjian, R., Skarnes, W. C., and Wang, Z. ES cell pluripotency and germ-layer formation require the SWI/SNF chromatin remodeling component BAF250a. Proc. Natl. Acad. Sci. 105, 6656–6661. doi: 10.1073/pnas.0801802105 (2008).

Gudmundsdottir, B. et al. POGZ is required for silencing mouse embryonic β-like hemoglobin and human fetal hemoglobin expression. Cell Rep. 23, 3236–3248 (2018).

Gunther et al., A set of proteins interacting with transcription factor Sp1 identified in a two-hybrid screening. Molecular and Cellular Biochemistry, 210: 131–142 (2000)

Helsmoortel et al. A SWI/SNF-related autism syndrome caused by de novo mutations in ADNP. Nat. Genet. 46, 380 ‑ 384 (2014).

Ho, L., Ronan, J., Wu, J., Staahl, B. T., Chen, L., Kuo, A., et al.An embryonic stem cell chromatin remodeling complex, esBAF, is essential for ESC self-renewal and pluripotency. Proc. Natl. Acad. Sci. 106, 5181–5186. doi: 10.1073/pnas.0812889106 (2008).

Ho et al. An embryonic stem cell chromatin remodeling complex, esBAF, is an essential component of the core pluripotency transcriptional network. PNAS, 106 (13):

5187 – 5191 (2009).

Ibaraki, K. et al. Expression analyses of POGZ, a responsible gene for neurodevelopmental disorders, during mouse brain development. Dev. Neurosci. 41, 139 – 148 (2019).

Kaya-Okur et al., CUT&Tag for efficient epigenomic profiling of small samples and single cells. NATURE COMMUNICATIONS, 10:1930, https://doi.org/10.1038/s41467-019-09982-5 (2019)

Kidder, B., Palmer, S., and Knott, J. SWI/SNF-Brg1 regulates self-renewal and occupies core pluripotency-related genes in embryonic stem cells. Stem. Cells, 27, 317–328. doi: 10.1634/stemcells.2008-0710 (2009).

King, H. W., and Klose, R. J. The pioneer factor OCT4 requires the chromatin remodeller BRG1 to support gene regulatory element function in mouse embryonic stem cells. eLife 6:e22631. doi: 10.7554/eLife.22631 (2017).

Ku, M., Koche, R. P., Rheinbay, E., Mendenhall, E. M., Endoh, M., Mikkelsen, T. S., et al. Genomewide analysis of PRC1 and PRC2 occupancy identifiifies two classes of bivalent domains. PloS Genet. 4:e1000242. doi: 10.1371/journal.pgen. 1000242 (2008).

Lei, L., West, J., Yan, Z. J., Gao, X., Fang, P., Dennis, J. H., et al. BAF250a protein regulates nucleosome occupancy and histone modifications in priming embryonic stem cell differentiation. J. Biol. Chem. 290, 19343–19352. doi: 10.1074/jbc.m115.637389 (2015).

Liu et al. Genome-wide studies reveal the essential and opposite roles of ARID1A in

controlling human cardiogenesis and neurogenesis from pluripotent stem cells. Genome Biology 21:169 (2020)

Loh et al. The Oct4 and Nanog transcription network regulates pluripotency in mouse embryonic stem cells. NATURE GENETICS, 38(4): 431-410. doi:10.1038/ng1760 (2006)

Mattout et al. Heterochromatin Protein 1β (HP1β) has distinct functions and distinct nuclear distribution in pluripotent versus differentiated cells. Genome Biology, 16:213 DOI: 10.1186/s13059-015-0760-8 (2015)

Ninkovic et al. The BAF Complex Interacts with Pax6 in Adult Neural Progenitors to Establish a Neurogenic Cross-Regulatory Transcriptional Network. Cell Stem Cell 13, 403–418 (2013)

Nozawa, R. et al. Human POGZ modulates dissociation of HP1alpha from mitotic chromosome arms through Aurora B activation. Nat. Cell Biol. 12, 719–727 (2010)

Ostapcuk, V. et al. Activity-dependent neuroprotective protein recruits HP1 and CHD4 to control lineage-specifying genes. Nature 557, 739 – 743 (2018).

Panamarova et al. The BAF chromatin remodelling complex is an epigenetic regulator of lineage specification in the early mouse embryo. Development 143, 1271-1283 doi:10.1242/dev.131961(2016)

Ran et al. Genome engineering using the CRISPR-Cas9 system. Nature protocols, 8: 2281. doi:10.1038/nprot. (2013)

Sanulli, S, MJ. Trnka, V. Dharmarajan, RW. Tibble, BD. Pascal, AL. Burlingame, PR. Griffin, JD. Gross, GJ. Narlikar. HP1 reshapes the nucleosome core to promote phase

separation of heterochromatin. Nature. 575(7782): 390–394. doi:10.1038/s41586-019-1669-2. (2019)

Sridharan R, Gonzales-Cope M, Chronis C, Bonora G, McKee R, Huang C, et al. Proteomic and genomic approaches reveal critical functions of H3K9 methylation and heterochromatin protein-1gamma in reprogramming to pluripotency. Nat Cell Biol. 15:872–82 (2013).

Stessman, H. A. F. et al. Disruption of POGZ is associated with intellectual disability and autism spectrum disorders. Am. J. Hum. Genet. 98, 541 – 552 (2016).

Sun et al. ADNP promotes neural differentiation by modulating Wnt/β-catenin signaling. NATURE COMMUNICATIONS, 11: 2984 https://doi.org/10.1038/s41467-020-16799-0 (2020)

Sun X, Yu W, Li L and Sun Y. ADNP Controls Gene Expression Through Local Chromatin Architecture by Association With BRG1 and CHD4. *Front. Cell Dev. Biol.* 8:553. doi: 10.3389/fcell.2020.00553 (2020)

Takebayashi et al. Murine esBAF chromatin remodeling complex subunits BAF250a and Brg1 are necessary to maintain and reprogram pluripotency-specific replication timing of select replication domains. Epigenetics & Chromatin 2013, 6:42 (2013)

Tan, B. et al. A novel de novo POGZ mutation in a patient with intellectual disability. J. Hum. Genet. 61, 357 – 359 (2016).

Vermeulen, M. et al. Quantitative interaction proteomics and genome-wide profifiling of epigenetic histone marks and their readers. Cell 142, 967 – 980 (2010).

Wang, X., Lee, R. S., Alver, B. H., Haswell, J. R., Wang, S., Mieczkowski, J., et al.

SMARCB1-mediated SWI/SNF complex function is essential for enhancer regulation. Nat. Genet. 49, 289–295. doi: 10.1038/ng. 3746 (2017).

White et al. POGZ truncating alleles cause syndromic intellectual disability. Genome Medicine 8: 3-11. DOI 10.1186/s13073-015-0253-0 (2016).

Xiong et al. Stemness factor Sall4 is required for DNA damage response in embryonic stem cells. J. Cell Biol. Vol. 208(5): 513–520 (2014)

Yang, P. Y., Oldfifield, A., Kim, T. Y., Yang, A., Yang, J. Y. H., Ho, J. W. K., et al. Integrative analysis identififies co-dependent gene expression regulation of BRG1 and CHD7 at distal regulatory sites in embryonic stem cells. Bioinformatics 33, 1916–1920. doi: 10.1093/bioinformatics/ btx092 (2017).

Ye et al. De novo POGZ mutations are associated with neurodevelopmental disorders and microcephaly. Cold Spring Harb Mol Case Stud. doi: 10.1101/mcs.a000455 (2015).

Zaidan and Sridharan. HP1 regulates H3K36 methylation and pluripotency in embryonic stem cells. Nucleic Acids Research, Vol. 48, No. 22: 12660–12674 (2020).

Zhang, X., Li, B., Li, W., Ma, L., Zheng, D., Li, L., et al. Transcriptional repression by the BRG1-SWI/SNF complex affects the pluripotency of human embryonic stem cells. Stem. Cell Rep. 3, 460–474. doi: 10.1016/j.stemcr. (2014).

Zhao et al., Rare inherited missense variants of POGZ associate with autism risk and disrupt neuronal development. Journal of Genetics and Genomics, 46: 247-257 (2019)

Acknowledgments. This work was supported by National Key Research and Development Program (2016YFA0101100), and National Natural Science Foundation of China (31671526) to YH Sun.

Author contributions. XY Sun performed the experiments; LX Cheng performed the bioinformatics analysis; YH Sun designed the work, provided the final support of the work, and wrote the paper.

Competing interests. The authors declared no competing interests.

Figure Legends

Fig. 1 POGZ depletion leads to loss of ESC phenotype. **a** Cartoon depicting the gRNA targeting sites at exon 2 of the mouse *Pogz* gene. **b** Genotyping showing the mutant allele 1 (Mut1) of *pogz*. **c** qRT-PCR showing the reduction of *Pogz* expression in mutant ESCs. **d** Western blot analysis of POGZ levels in control and *Pogz-/-* ESCs. The WB has been repeated at least three times. **e** Double IF staining of OCT4 and POGZ showing that OCT4 levels were not significantly altered in early passaging mutant ESCs. Similar results were obtained for NANOG (not shown). **f** The cell growth cure showing the proliferation defects of *Pogz-/-* and *Pogz+/-* ESCs compared to control ESCs. **g** Representative image showing morphology of control and late passaged *Pogz-/-* ESCs. White arrows pointing to differentiated cells. **h** Alkaline phosphotase staining showing the compromised ESC stemness in *Pogz-/-* ESCs. White arrows pointing to cells with reduced AP activities. **i** The mRNA expression

levels of representative pluripotency-related, mesodermal, neuroectodermal, endodermal genes in control and *Pogz-/-* ESCs. qRT-PCR has been repeated at least three times. **j** IF staining of GATA6 showing that GATA6 was abnormally expressed in *Pogz-/-* ESCs, but not expressed in control ESCs. Restoring POGZ rescued the abnormal expression of Gata6. **k** WB showing that OCT4 levels were reduced in late passaging *Pogz-/-* ESCs, which can be reversed by restoring POGZ. **l** Valcano plot showing the up- and down-regulated genes in the control and *Pogz-/-* ESCs. The RNA-seq experiments were repeated two times. The numbers of DEGs were shown as average. **m** GO analysis of DEGs between control and *Pogz-/-* ESCs. **n** KEGG analysis of DEGs for control and *Pogz-/-* ESCs. Significant levels are: **p*< 0.05; ***P*< 0.01; ****P*< 0.001; NS: not significant. Bar: 25 μm.

Supplementary Fig. 1 Related to Figure 1. **a** Genotyping showing two additional mutant alleles: 2 and 3 (Mut2/3). **b** PH3 staining of control and *Pogz-/-* ESCs, showing decreased number of PH3 positive cells in *Pogz-/-* ESCs. **c** Quantification of (**b**), by measuring fluorescence intensity. **d** IF staining of GATA6 showing that GATA6 protein was ectopically expressed in two additional *Pogz-/-* ESC lines, but not in control ESCs. Bar: 25 μm.

Fig. 2 Loss of POGZ leads to compromised ESC pluripotency. **a** Morphology of day 1, 3 and 6 EBs from control and mutant ESCs. **b** qRT-PCR analysis showing the dynamic expression of pluripotency, endodermal, mesodermal and neuroectodermal genes during 8-day of EB formation. **c** Valcano plot showing the up- and down-regulated genes (fold change >2) between day 6 EBs from control and *Pogz-/-*

ESCs. The RNA-seq experiments were repeated three times. The numbers of up- and down-regulated genes were shown as average. **d** GO analysis of down-regulated DEGs of day 6 EBs from control and *Pogz-/-* ESCs. **e** KEGG analysis of down-regulated DEGs of day 6 EBs from control and *Pogz-/-* ESCs. **f** Heat map analysis of representative neuroectodermal and pluripotency genes. Significant levels are: *$p< 0.05$; **$P< 0.01$; NS: not significant. Bar: 25 μm.

Supplementary Fig. 2 Related to Figure 2. **a** Morphology of day 1, 2, 6 and 8 EBs from control and two additional *Pogz* mutant ESCs (Mut2/3). ESC EB formation experiments were repeated at least two times. Bar: 25 μm.

Fig. 3 POGZ associates with esBAF/BRG1 and HP1. **a** Left: Cartoon showing the IP followed Mass Spec experiment. Right: the identified POGZ interacting proteins. **b** Co-IP results confirming the interaction between POGZ and BAF155 or HP1γ in ESCs. **c** Co-IP results showing the interaction between POGZ and BRG1 in ESCs. **d** Direct interaction of in vitro synthesized POGZ and BRG1 proteins. POGZ and FLAG-BRG1 proteins were synthesized using a rabbit reticulocyte lysate system. **e** Diagram showing the various truncated forms of BRG1 and POGZ. **f** Co-IP results showing that the N-terminal of BRG1 interacts with POGZ in 293T cells. **g** Co-IP results showing that the N-terminal of BRG1 interacts with the N-terminal of POGZ in 293T cells. **h** Sequential IP experiments showing that POGZ, BRG1 and HP1γ can for a triplex in ESCs. *: non-specific band. **i** Cartoon showing the PBH triplex. All experiments were repeated at least two times, and shown are representative images.

Supplementary Fig. 3 Related to Figure 3. **a** Double IF staining of HP1γ and POGZ.

b Direct interaction of in vitro synthesized POGZ and BAF155. **c** Double IF staining of BRG1 and POGZ. **d** and **e** Co-IP results showing that the C-terminal and middle fragments of BRG1 did not interact with POGZ. All experiments were repeated at least two times, and shown are representative images

Fig. 4 POGZ binding profile genome-wide based on CUT&Tag and ChIP-seq. **a** Pie chart showing the binding features of POGZ genome wide. **b** A metaplot of POGZ CUT&Tag signals at the POGZ peak center. Similar results were obtained by ChIP-seq. **c** A metaplot of POGZ CUT&Tag signals at TSS. Similar results were obtained by ChIP-seq. **d** GO analysis of POGZ-bound targets in ESCs. **e** KEGG analysis of POGZ-bound targets in ESCs. **f** The KLF and OCT4/NANOG binding motifs revealed by HOMER. **g** ChIP-seq snapshots showing the co-localization of POGZ, NANOG and OCT4. Grey: proximal promoter; Orange: gene distal regions. **h** ChIP-seq signals of BRG1, NANOG and OCT4 with POGZ. **i** A venn diagram showing the overlapping binding sites among POGZ, BRG1, NANOG and OCT4. **j** ChIP snapshots at *Nanog* and *Pou5f1* loci showing a broad overlapping occupancy of POGZ, BRG1, OCT4, NANOG, H3K27Ac and MED1 (> 5kb), which was analogous to the previously described super-enhancers. Grey: proximal promoter; Orange: gene distal regions. **k** Double IF staining of OCT4 and POGZ. **l** Co-IP results showing that OCT4 interacts with POGZ in ESCs. All IF and WB experiments were repeated at least two times, and shown are representative images. Bar: 25 μm.

Supplementary Fig. 4 Related to Figure 4. **a** Snapshots at *Chchd1* and *Dcpl1a* loci showing that CUT&Tag performs better than FLAG ChIP-seq, including signal

intensity and peak numbers. Grey: proximal promoter; Orange: gene distal regions. **b** Snapshots at the indicated loci showing that POGZ is extensively localized to poised and active enhancer regions, decorated with H3K4me1 and H3K27Ac, respectively. Grey: proximal promoter; Orange: gene enhancer regions. Note the super-enhancers at *Nanog* and *Pax6* loci. **c** A panel of motifs of POGZ binding sites identified by HOMER. Shown were the top 18 motifs.

Fig. 5 POGZ, BRG1 and HP1 are co-localized genomewide. **a** A heat map view of ChIP-seq signals of POGZ, BRG1, HP1β/CBX1 and HP1γ/CBX3 at POGZ peaks. **b** A metaplot showing that BRG1 and HP1γ occupancy at POGZ-peak center (Up), and at POGZ-bound TSS regions (Bottom). **c** The overlapping of ChIP-seq sites among POGZ, BRG1 and HP1γ genome wide. **d** GO analysis of PBH-bound genes (Up), and KEGG analysis of PBH-bound targets (Bottom). **e** A heat map view for distribution of POGZ, BRG1 and HP1γ/CBX3 signals in a ± 3 kb regions around the TSS. Genes therefore are classified into 7 sub-groups based on the occupancy of POGZ, BRG1 and HP1γ. **f** The relative expression levels of the indicated classified genes, based on (**e**). **g** The effects of loss of POGZ on the expression of the classified genes. **h** ChIP analysis showing that BRG1 and HP1γ/CBX3 levels were greatly reduced at pluripotency-, neural- and endodermal- genes, in the absence of POGZ. **i** A Pearson correlation analysis of ChIP-seq peaks revealed a high degree of co-localization of POGZ, BRG1, HP1, NANOG and OCT4 genome wide. **j** ChIP-seq snapshots showing the co-localization of POGZ, BRG1, HP1γ, NANOG and OCT4 at the indicated gene loci. Grey: proximal promoter; Orange: gene enhancer regions. **k** A

Venn diagram showing the up-regulated and down-regulated genes (fold change> 2, and $P< 0.05$) between *Pogz-/-* and HP1 triple KO ESCs. Left: up-regulated genes; right: down-regulated genes.

Supplementary Fig. 5 Related to Figure 5. **a** A Venn diagram showing the shared ChIP-seq peaks among POGZ, BRG1, HP1γ/CBX3 and HP1β/CBX1. **b** ChIP-seq snapshots showing the co-localization of POGZ, BRG1 and HP1γ/CBX3 at TSS (grey color) and distal enhancers (orange). **c** ChIP analysis using BRG1 antibodies for component genes of Wnt and Hippo signaling pathways. BRG1 levels were greatly reduced in the absence of POGZ. **d** A Venn diagram showing the shared ChIP-seq sites among POGZ, BRG1, OCT4, NANOG, HP1γ/CBX3 and HP1β/CBX1. **e** A Venn diagram showing the shared up-regulated and down-regulated genes (fold change> 2, and $P< 0.05$) among *Pogz-/-, Brg1-/-* and HP1 triple KO ESCs. Left: up-regulated genes; right: down-regulated genes. **f** ChIP-seq snapshots showing the co-localization of POGZ with esBAF components, such as BRG1, SS18 and BAF250a, at TSS (grey color) and distal enhancers (orange). **g** ChIP-seq snapshots showing that POGZ is extensively co-localized with H3K4me1 and H3K27Ac, but not with repressive marks H2Aub1 and H3K27me3 at distal enhancers. Note that a small but significant POGZ levels were observed at TSS of *Gata6* where H2Aub1 and H3K27me3 were deposited.

Fig. 6 POGZ regulates chromatin accessibility by association with BRG1. **a** A metaplot showing the reduced chromatin accessibility at POGZ-peak center in *Pogz-/-* ESCs compared to control ESCs. **b** Snapshots of a randomly selected genomic region

in chromosome 18 showing that the chromatin accessibility was reduced in the absence of POGZ at many POGZ and BRG1 bound sites. **c** Snapshots of the indicated gene loci showing that the chromatin accessibility was reduced in the absence of POGZ at POGZ and BRG1 co-bound sites, at TSS (grey color) and distal enhancer (orange) regions. **d** A metaplot showing that BRG1 ChIP-seq peaks are more enriched at POGZ-dependent ATAC peaks. **e** At POGZ-dependent sites where ATAC-seq signals were greatly reduced in the absence of POGZ, loss of BRG1 also showed reduction in chromatin accessibility. **f** A metaplot showing the increased nucleosome occupancy in *Pogz-/-* ESCs compared to control ESCs. **g** Close-up snapshots showing the change of nucleosome occupancy and phasing at the indicated gene loci. **h** Comparison analysis of global expression for POGZ-bound genes that exhibit altered chromatin accessibility, in control and *Pogz-/-* ESCs. **i** Cartoon showing the function of POGZ in ESCs. PBH triplex have a dual function: facilitating ESC-specific genes and suppressing lineage-specifying genes.

Supplementary Fig. 6 Related to Figure 6. **a** The top three binding motifs in sites where ATAC-seq signals were altered in the absence of POGZ by HOMER. **b** Snapshots of the indicated gene loci showing that the chromatin accessibility was reduced in the absence of POGZ at POGZ and BRG1 co-bound sites. Grey color for TSS and orange for distal enhancers. **c** Snapshots of ATAC-seq signals at the indicated gene loci, showing that chromatin accessibility was similarly reduced in the absence of POGZ, BRG1 and OCT4. **d** Heat map showing that ATAC-seq signals were similarly reduced in POGZ- and BRG1-depleted ESCs, genome wide.

Figure 1. Depletion of POGZ in ESCs leads to loss of stemness

a

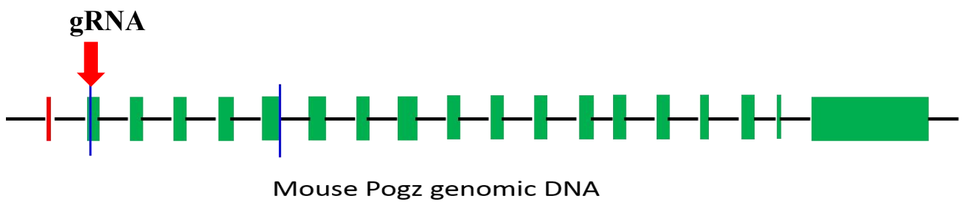

b

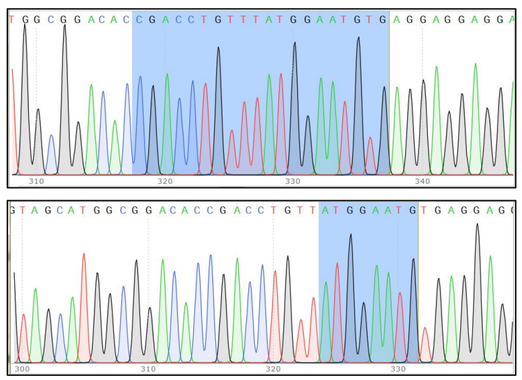

Control: GTAGCATGGCGGACACCGACCTGTTTATGGAATGTGAGG
Mut1 (-1bp): GTAGCATGGCGGACACCGACCTGTT*ATGGAATGTGAGG

c

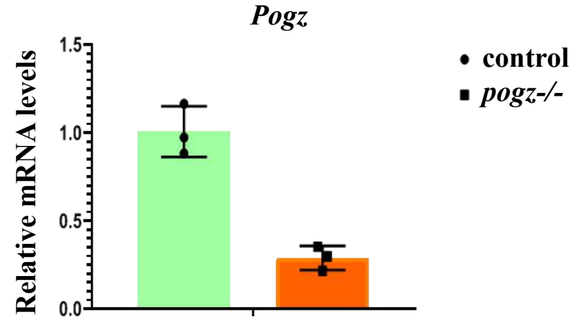

d

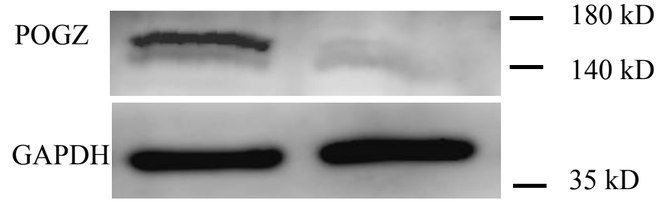

e

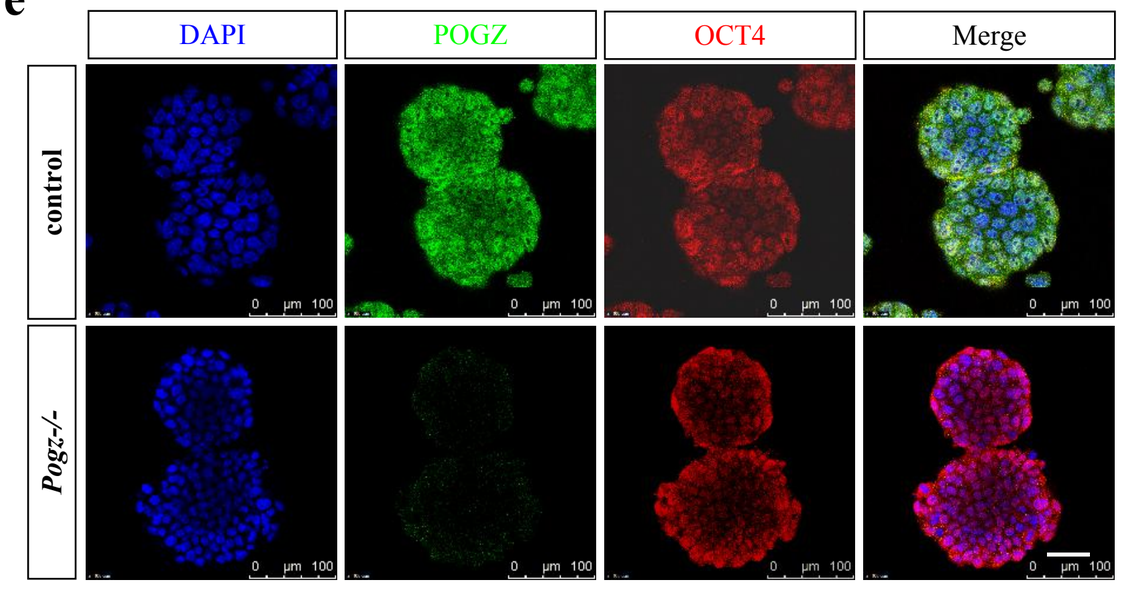

f

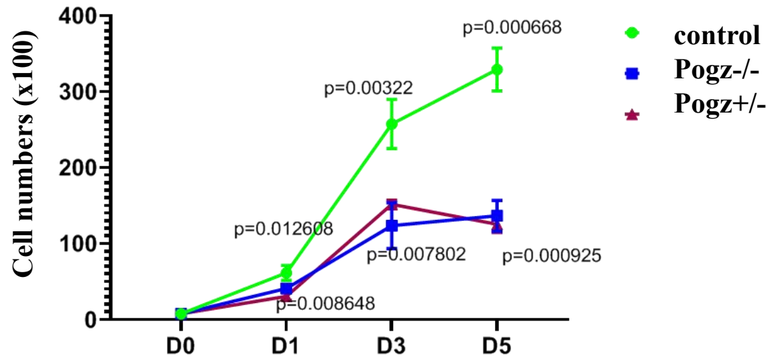

g

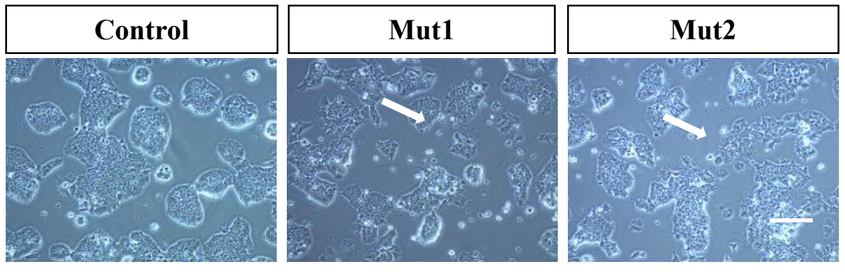

h

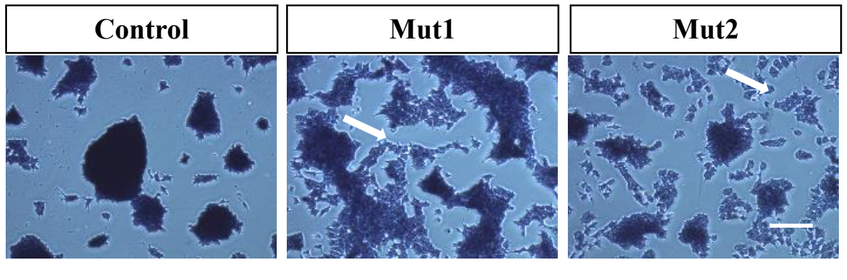

i

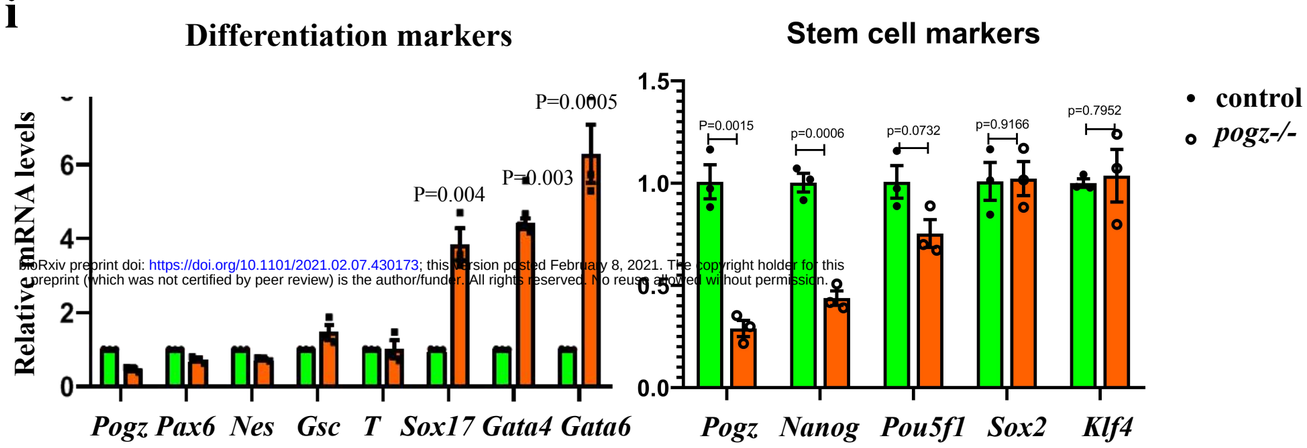

j

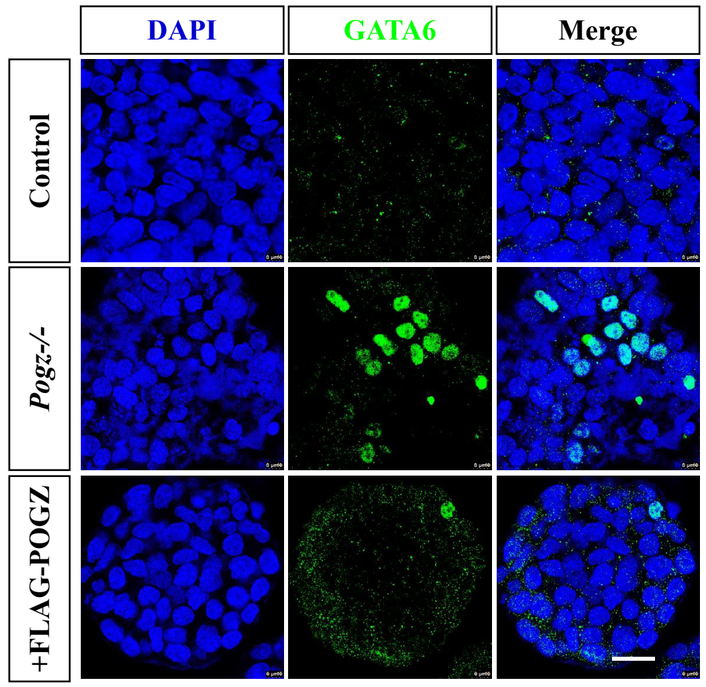

k

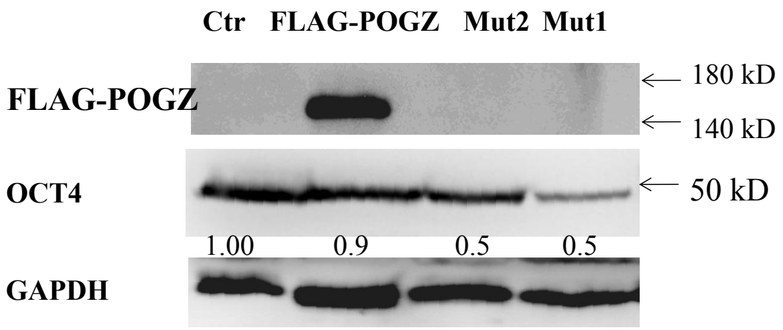

l

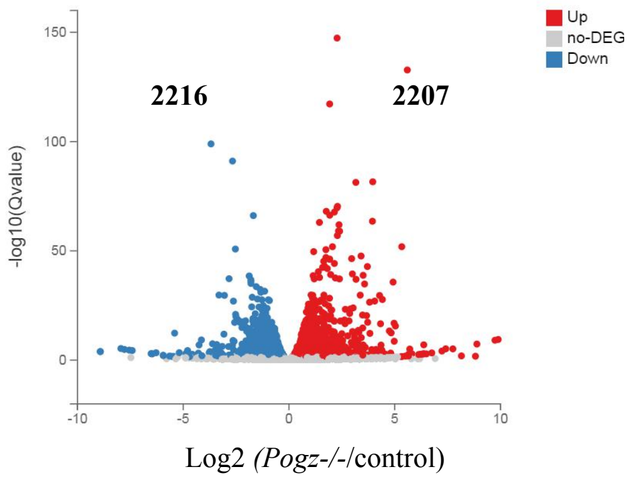

m

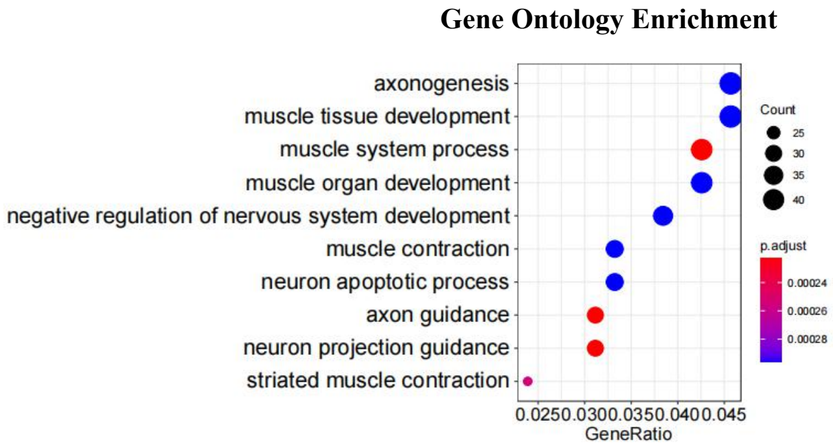

n

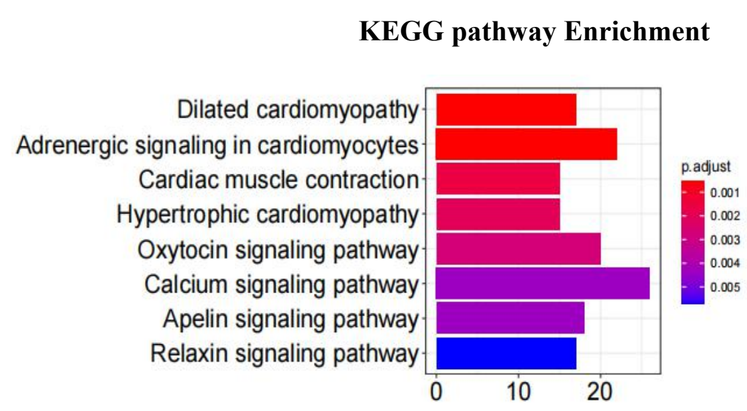

Supplementary Figure 1

a

P1-11 (Mut2)

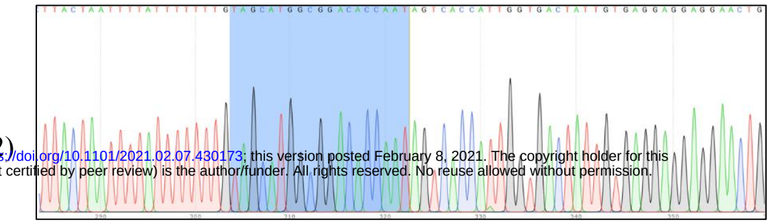

>control

TAGCATGGCGGACACCGAC***CTGTTTATGG**AATGTGAGGAGGAGGA**

>Mut2（+7bp）

TAGCATGGCGGACACCAATAGTCACCATTGGTGACTAATGTGAGGAGGAGGA

M2 (Mut3)

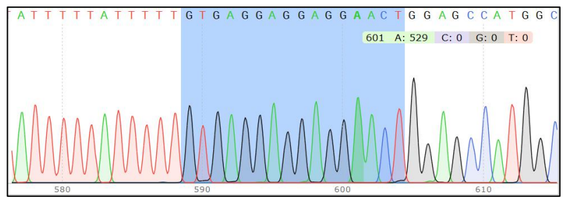

Control: GTAGCATGGCGGACACCGACCTGTTTATGGAATGTGAGG

Mut3 (+284bp): GTAGCATGGCGGACACCGACCTGTTTATGGAAT+…+GTGAGG

b

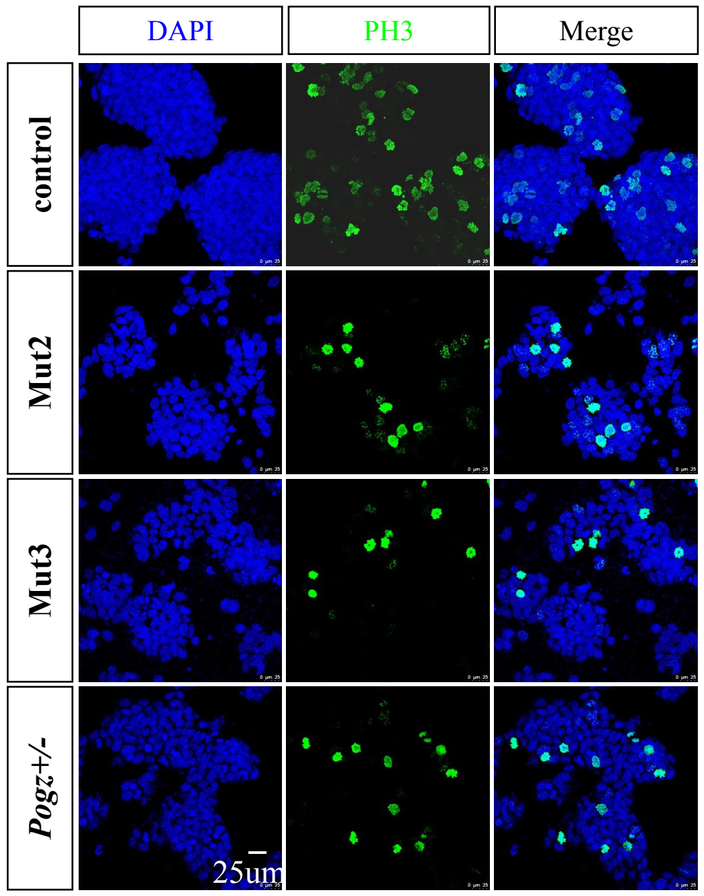

c

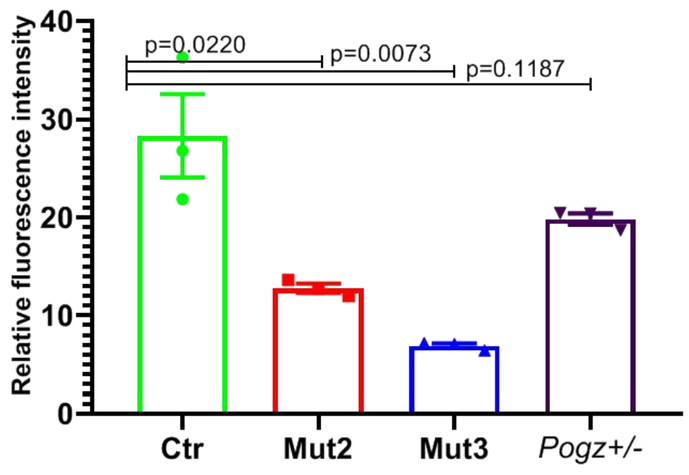

d

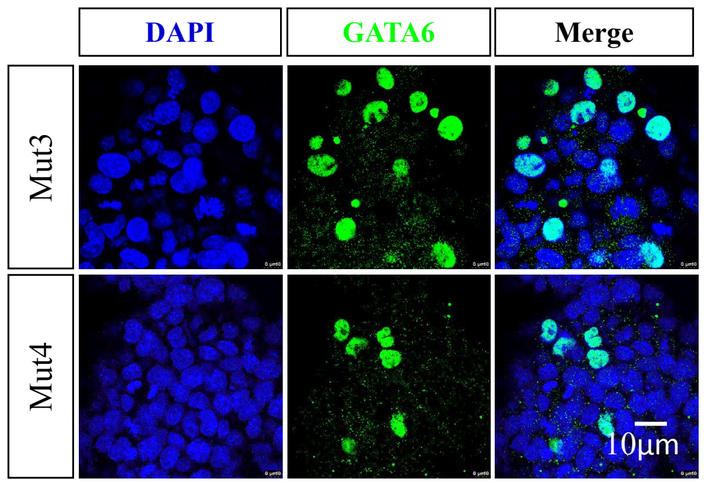

Figure 2. Loss of POGZ leads to compromised ESC pluripotency

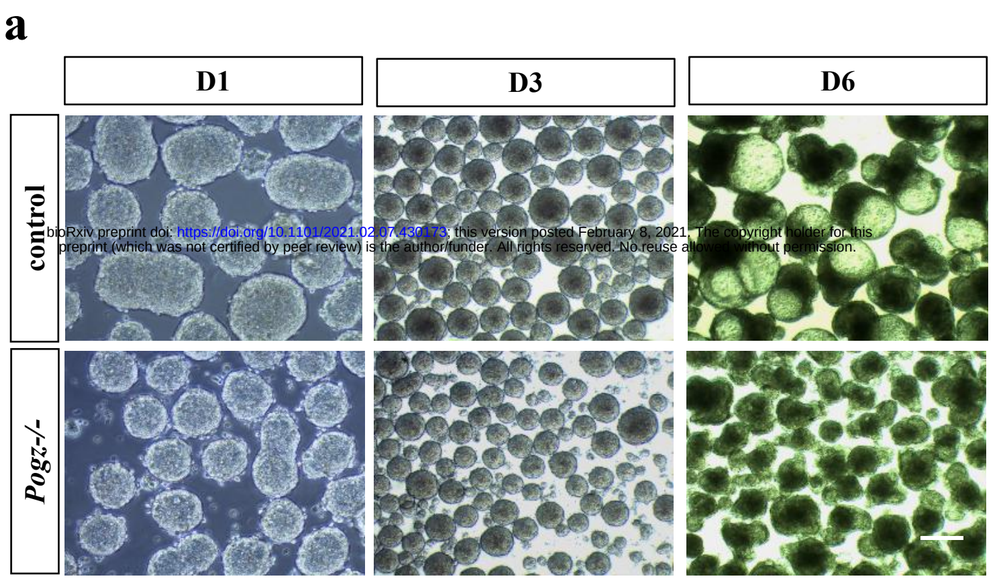

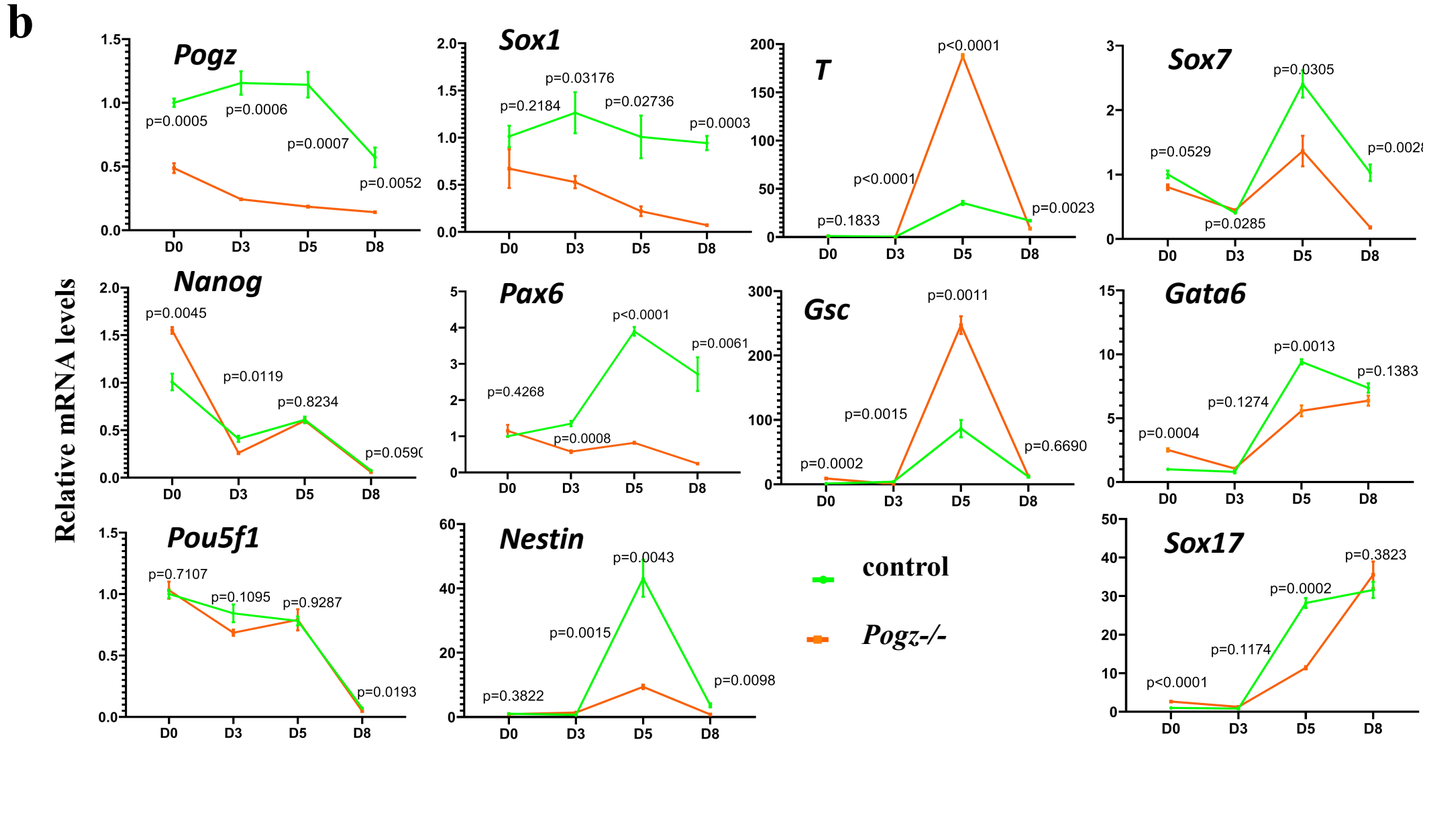

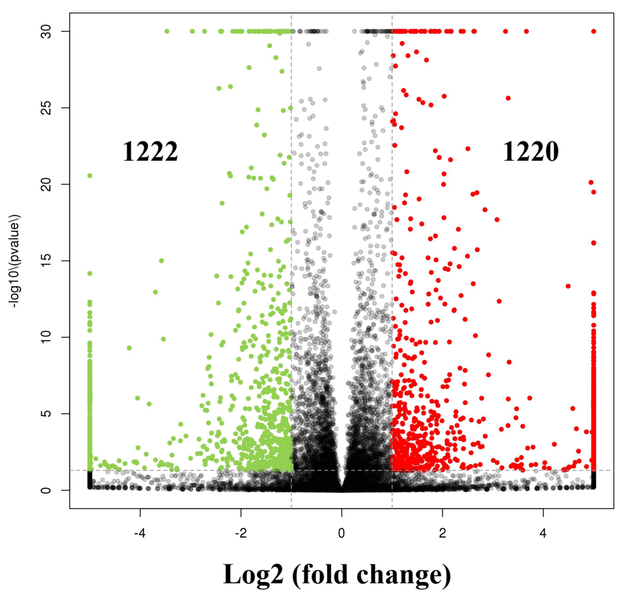

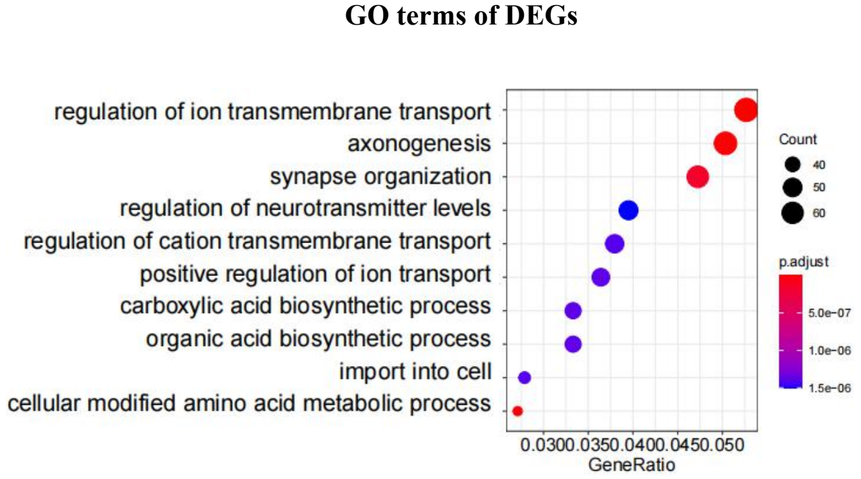

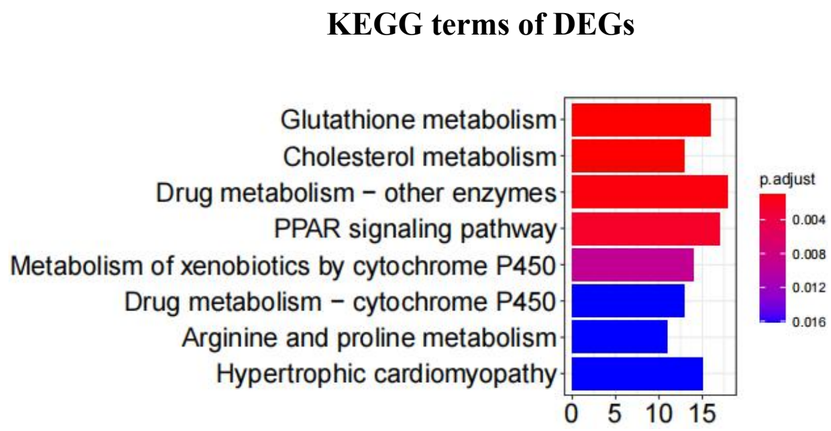

f

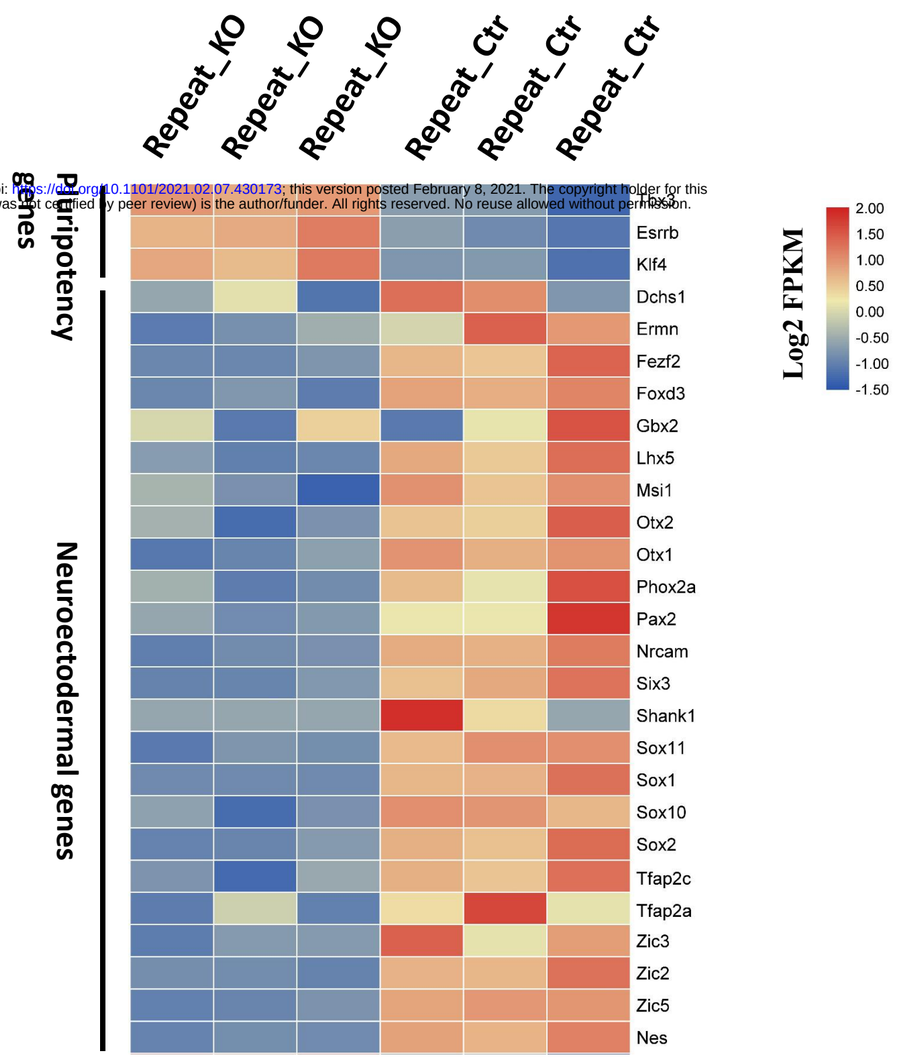

Supplementary Figure 2

a

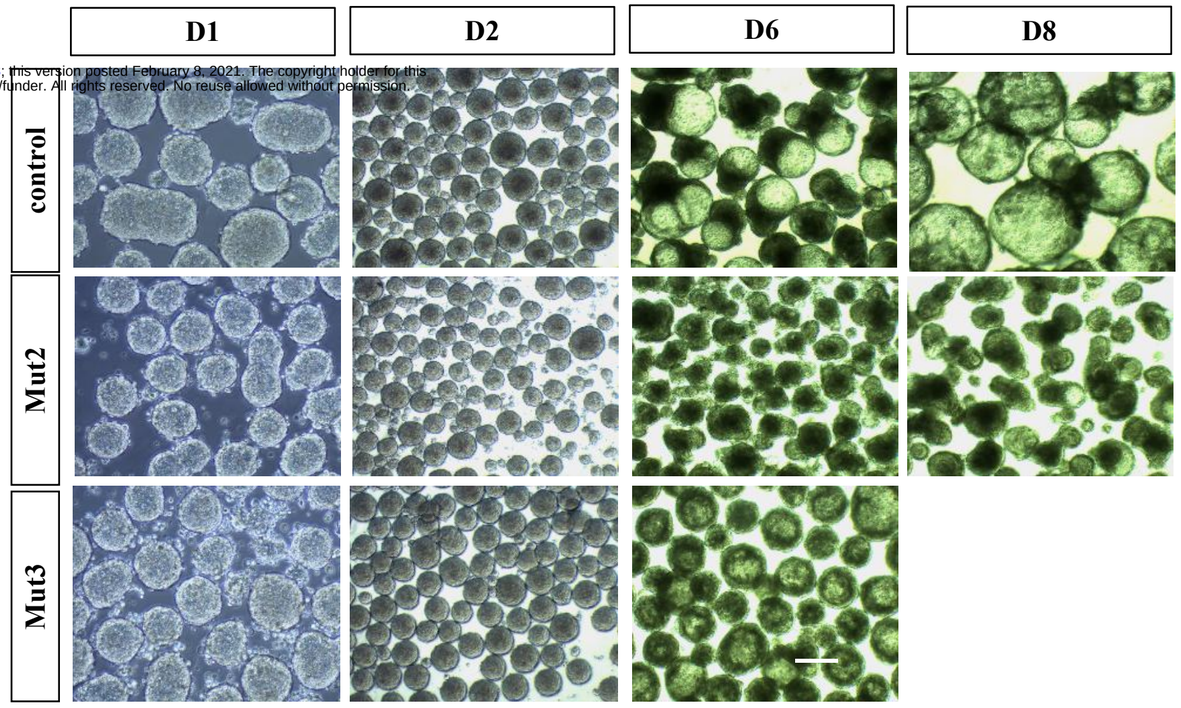

Figure 3 POGZ associates with esBAF and HP1

Supplementary Figure 3

a

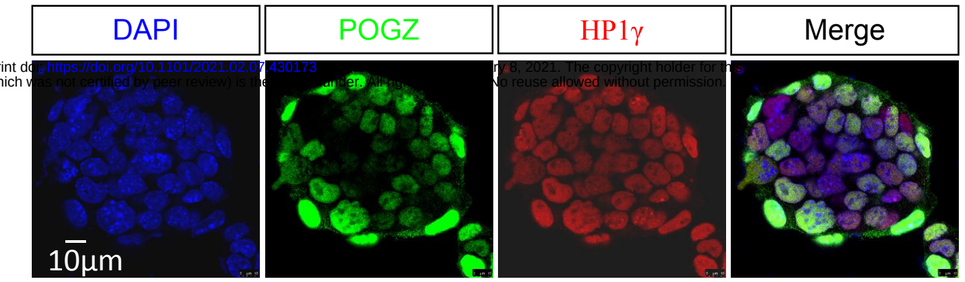

c

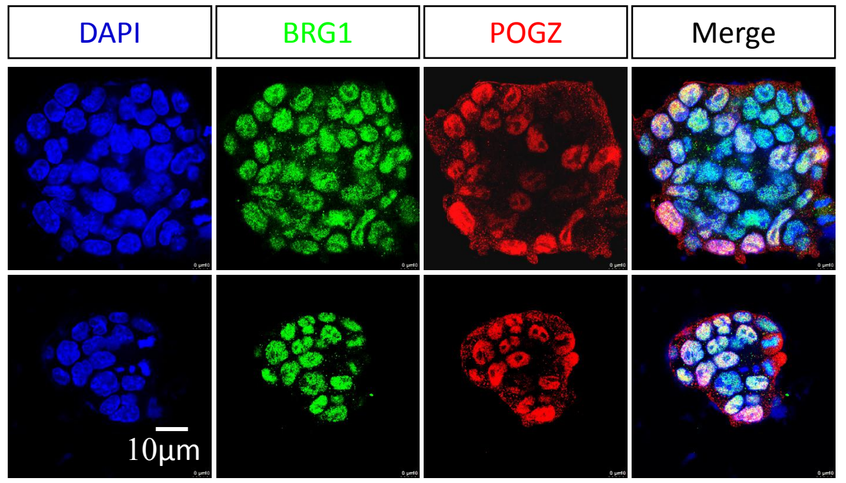

b

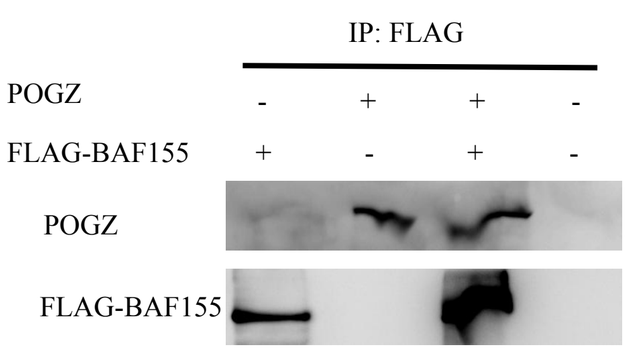

d

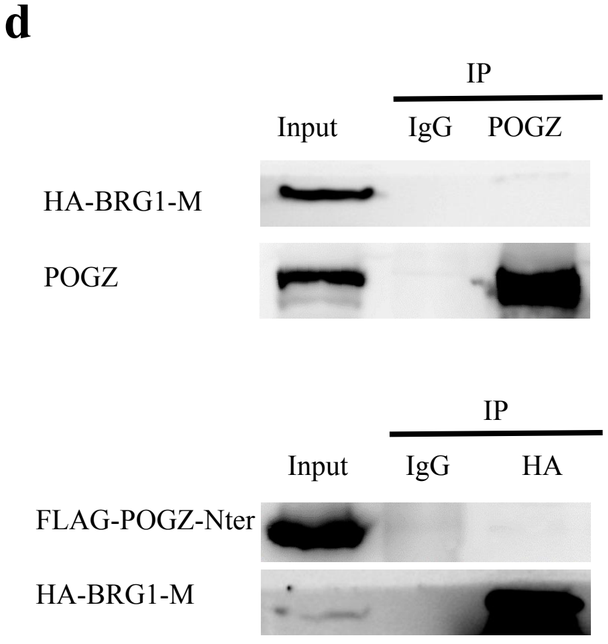

e

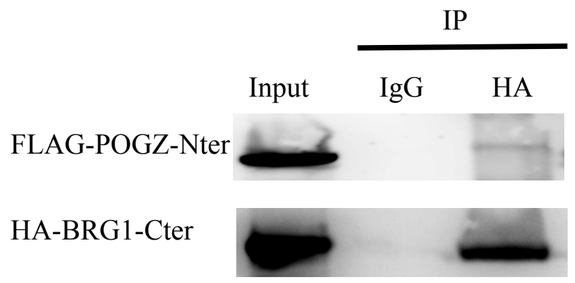

Figure 4 POGZ binding profile genome-wide

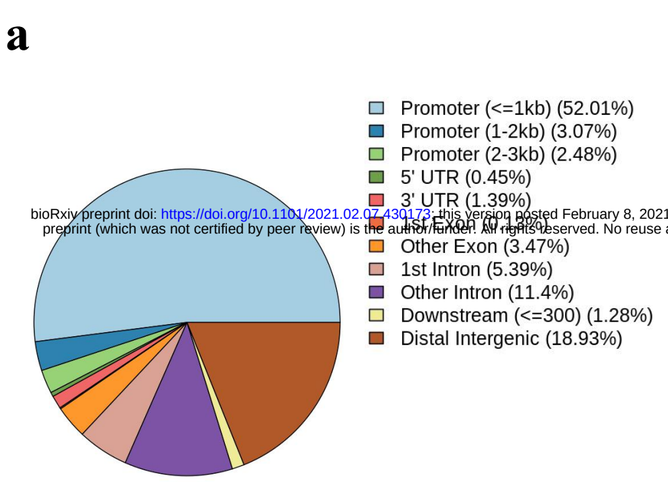

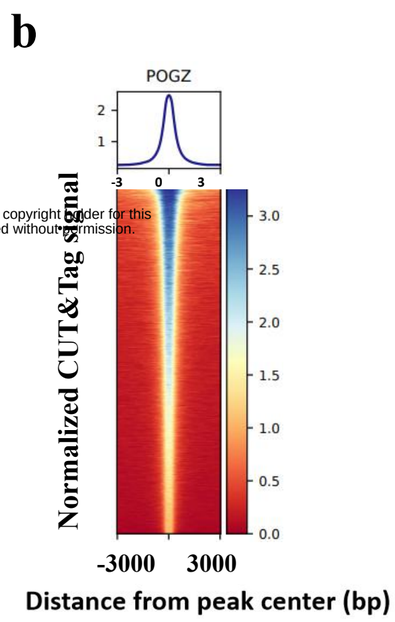

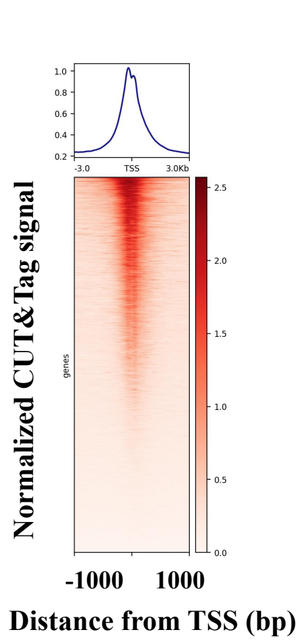

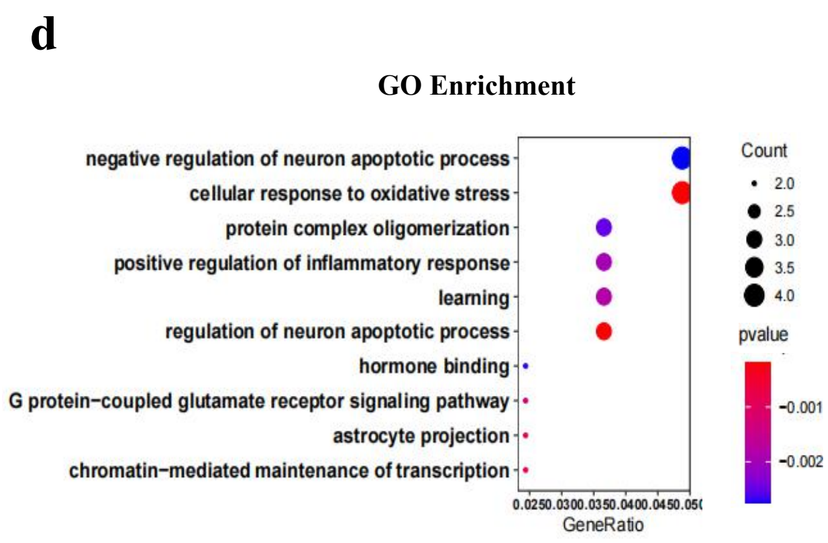

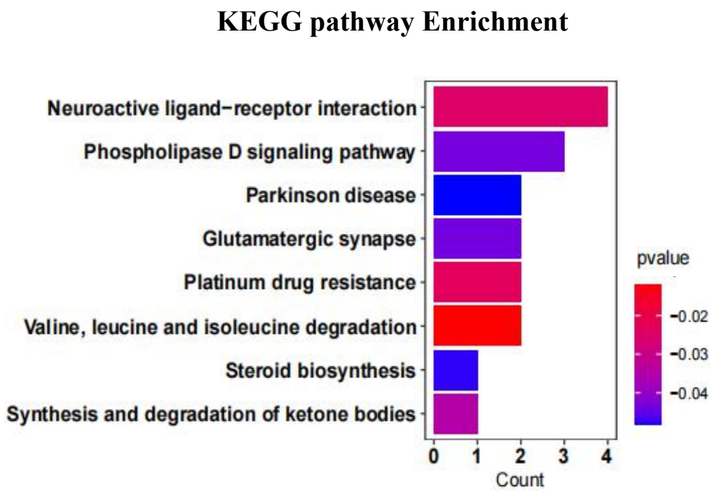

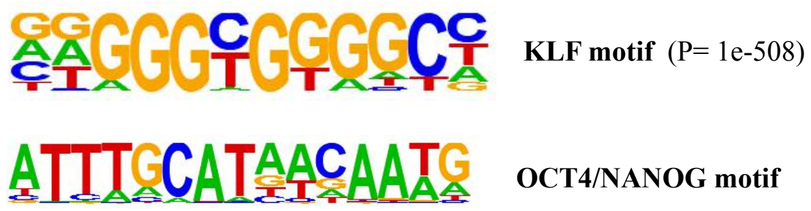

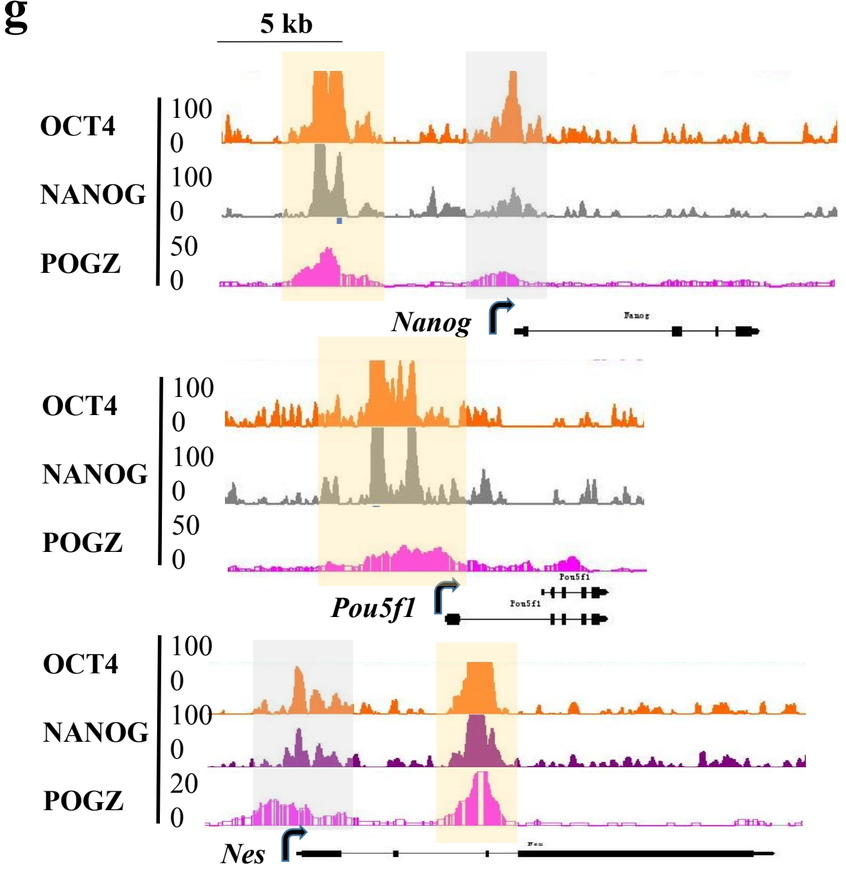

h

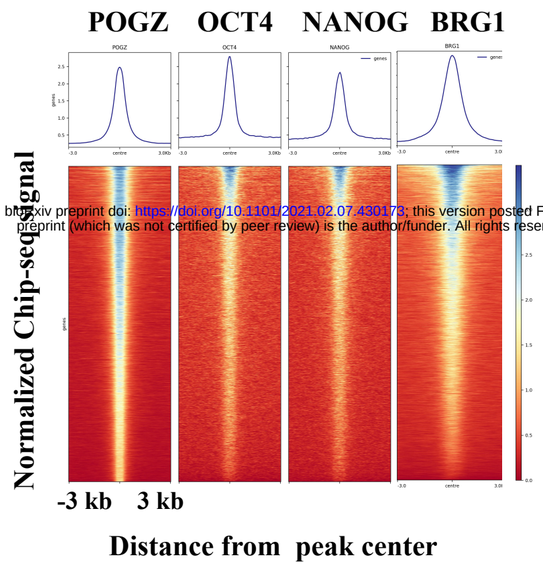

i

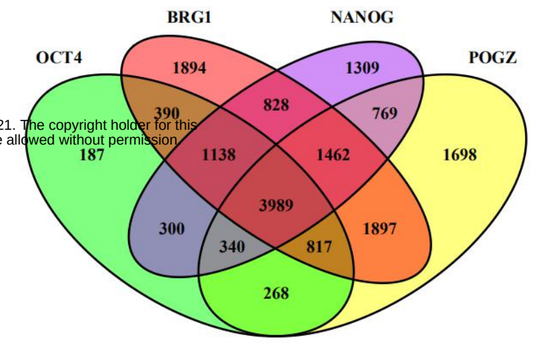

j

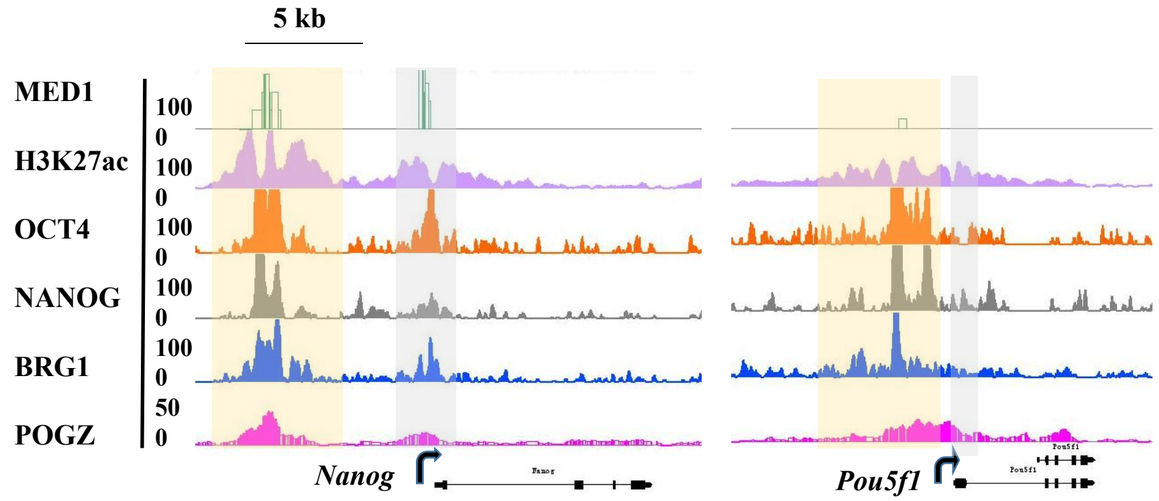

k

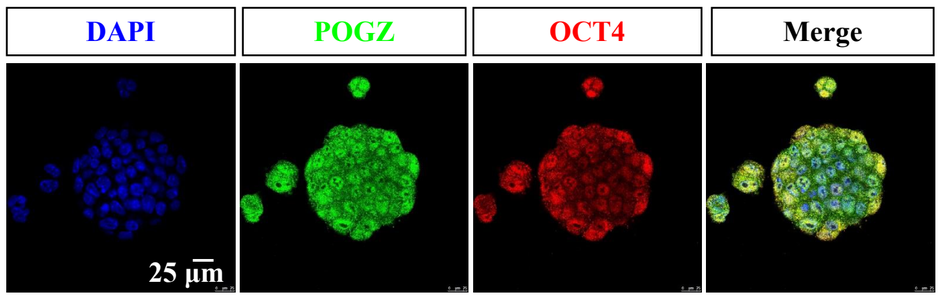

l

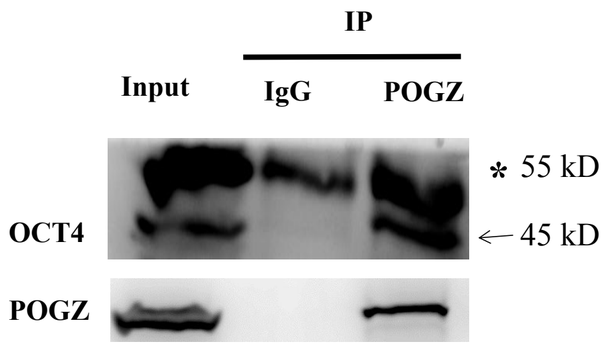

Supplemenyary Figure 4

a

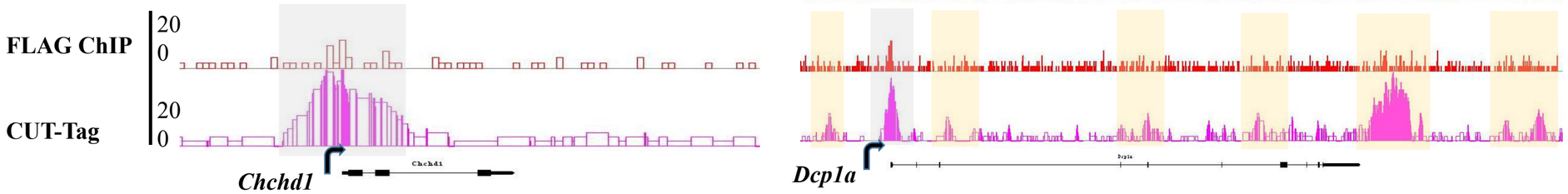

b

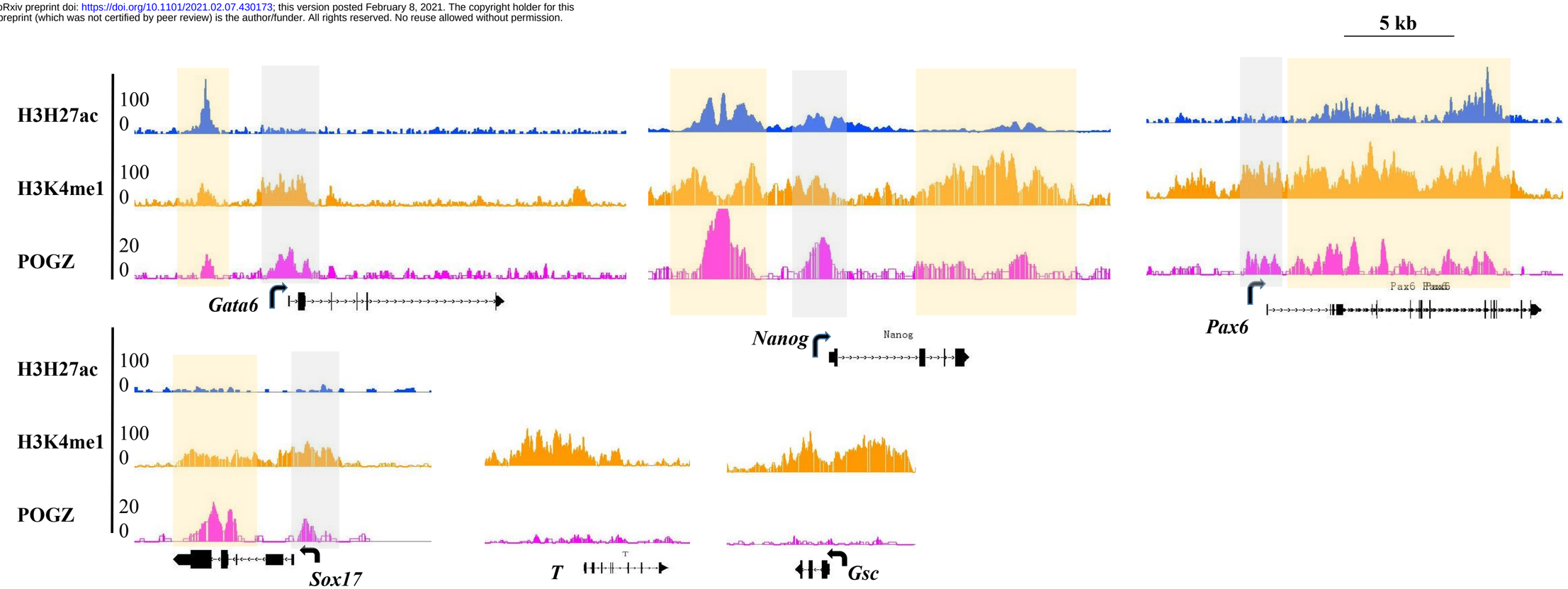

c

1		KLF1(Zf)/HUDEP2-KLF1-CutnRun(GSE136251)/Homer	1e-508	-1.170e+03	0.0000	4845.0	28.96%
2		Sp2(Zf)/HEK293-Sp2.eGFP-ChIP-Seq(Encode)/Homer	1e-421	-9.706e+02	0.0000	6418.0	38.37%
3		KLF3(Zf)/MEF-Klf3-ChIP-Seq(GSE44748)/Homer	1e-412	-9.506e+02	0.0000	3127.0	18.69%
4		Sp5(Zf)/mES-Sp5.Flag-ChIP-Seq(GSE72989)/Homer	1e-407	-9.379e+02	0.0000	5089.0	30.42%
5		KLF5(Zf)/LoVo-KLF5-ChIP-Seq(GSE49402)/Homer	1e-368	-8.494e+02	0.0000	5599.0	33.47%
6		Sp1(Zf)/Promoter/Homer	1e-318	-7.336e+02	0.0000	2425.0	14.50%
7		Klf4(Zf)/mES-Klf4-ChIP-Seq(GSE11431)/Homer	1e-271	-6.244e+02	0.0000	1976.0	11.81%
8		KLF14(Zf)/HEK293-KLF14.GFP-ChIP-Seq(GSE58341)/Homer	1e-249	-5.743e+02	0.0000	6685.0	39.96%

9		Klf9(Zf)/GBM-Klf9-ChIP-Seq(GSE62211)/Homer	1e-239	-5.505e+02	0.0000	2343.0	14.01%
10		KLF6(Zf)/PDAC-KLF6-ChIP-Seq(GSE64557)/Homer	1e-238	-5.489e+02	0.0000	4523.0	27.04%
11		Ronin(THAP)/ES-Thap11-ChIP-Seq(GSE51522)/Homer	1e-149	-3.437e+02	0.0000	267.0	1.60%
12		Elk4(ETS)/Hela-Elk4-ChIP-Seq(GSE31477)/Homer	1e-148	-3.425e+02	0.0000	2240.0	13.39%
13		KLF10(Zf)/HEK293-KLF10.GFP-ChIP-Seq(GSE58341)/Homer	1e-134	-3.093e+02	0.0000	2261.0	13.52%
14		EKLF(Zf)/Erythrocyte-Klf1-ChIP-Seq(GSE20478)/Homer	1e-124	-2.869e+02	0.0000	820.0	4.90%
15		GFY-Staf(?,Zf)/Promoter/Homer	1e-115	-2.662e+02	0.0000	323.0	1.93%
16		SUT1?/SacCer-Promoters/Homer	1e-114	-2.628e+02	0.0000	13319.0	79.62%
17		SeqBias: CG bias	1e-106	-2.456e+02	0.0000	15209.0	90.92%
18		OCT4-SOX2-TCF-NANOG(POU,Homeobox,HMG)/mES-Oct4-ChIP-Seq(GSE11431)/Homer	1e-105	-2.424e+02	0.0000	505.0	3.02%

Figure 5 POGZ, BRG1 and HP1 are co-localized genomewide

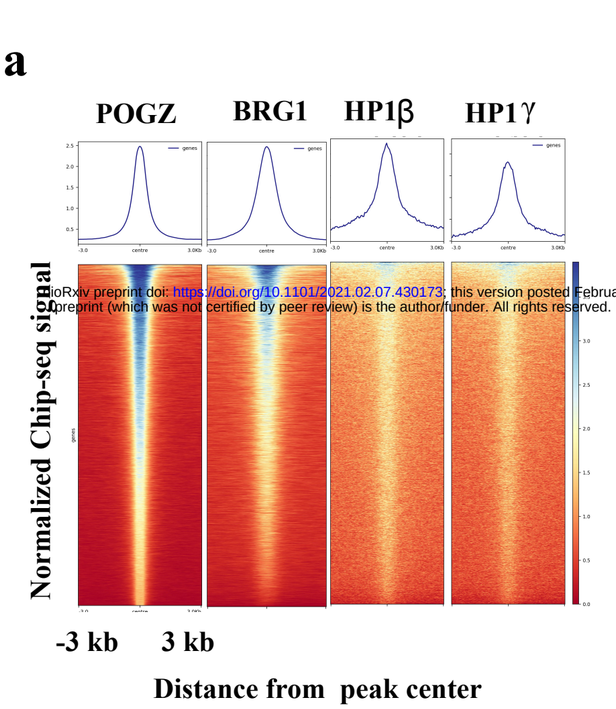

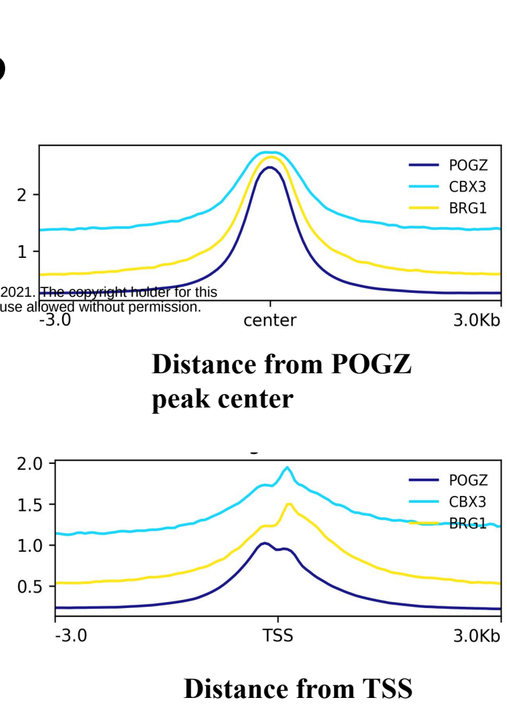

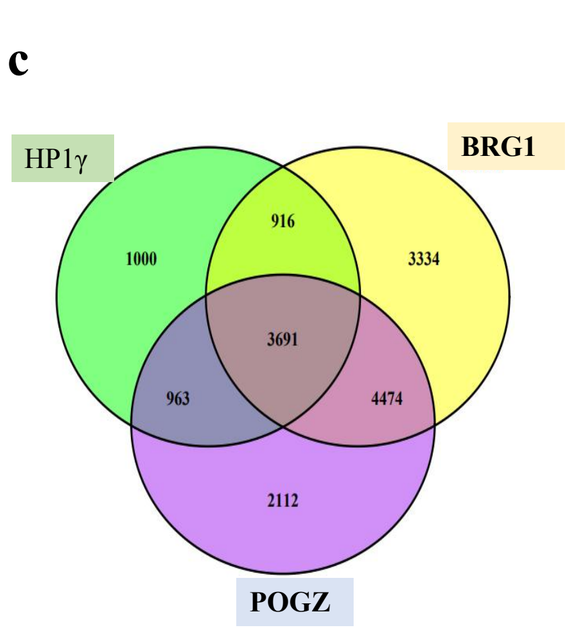

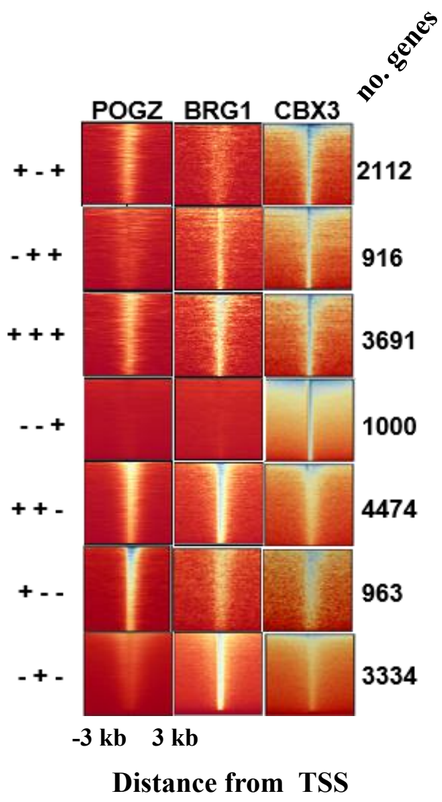

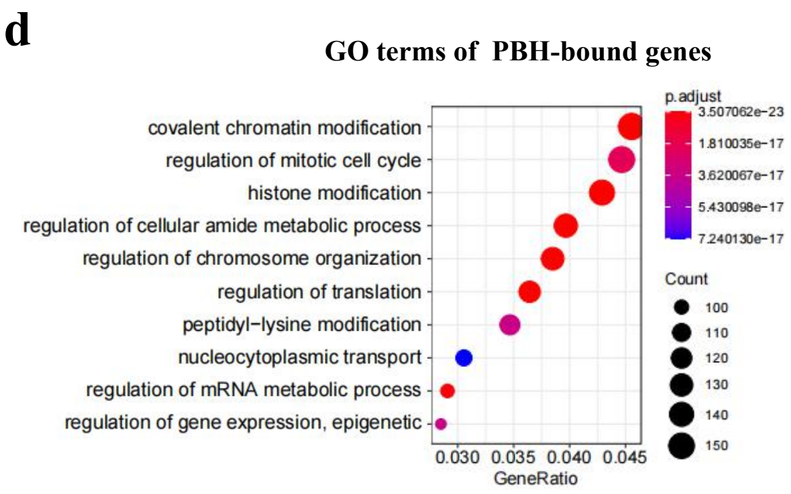

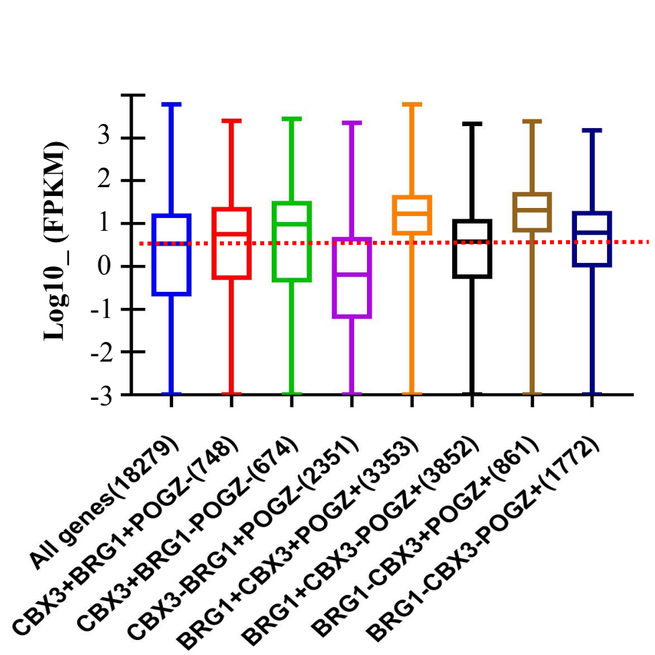

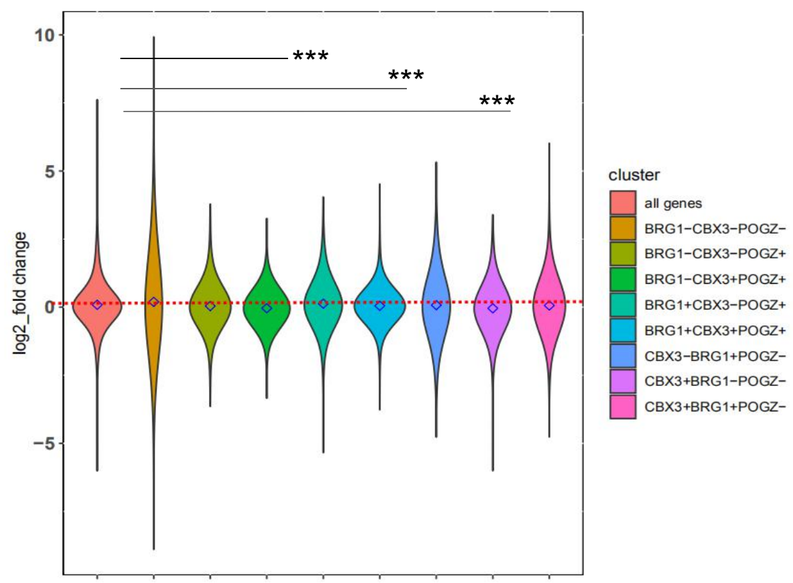

h

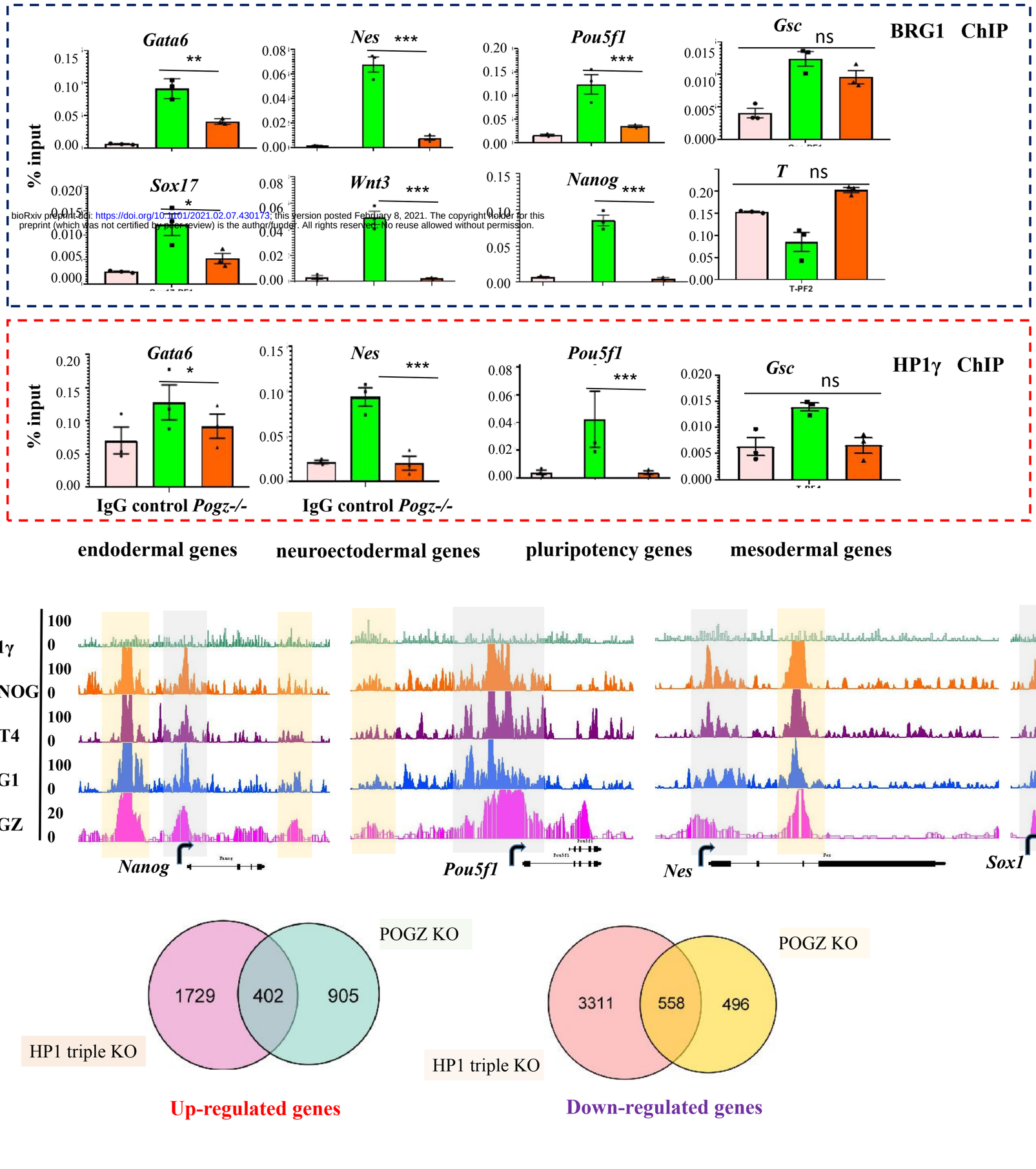

i

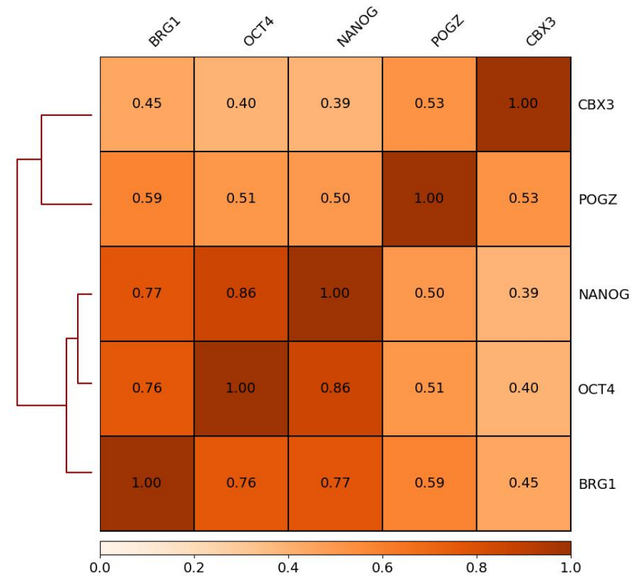

j

k

Supplementary Figure 5

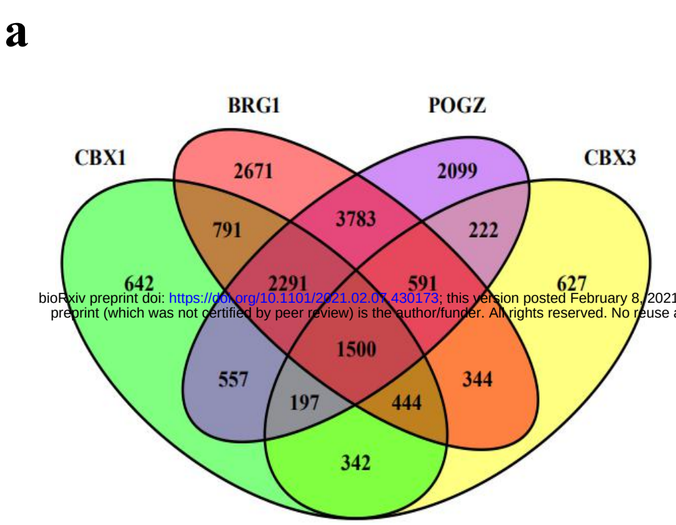

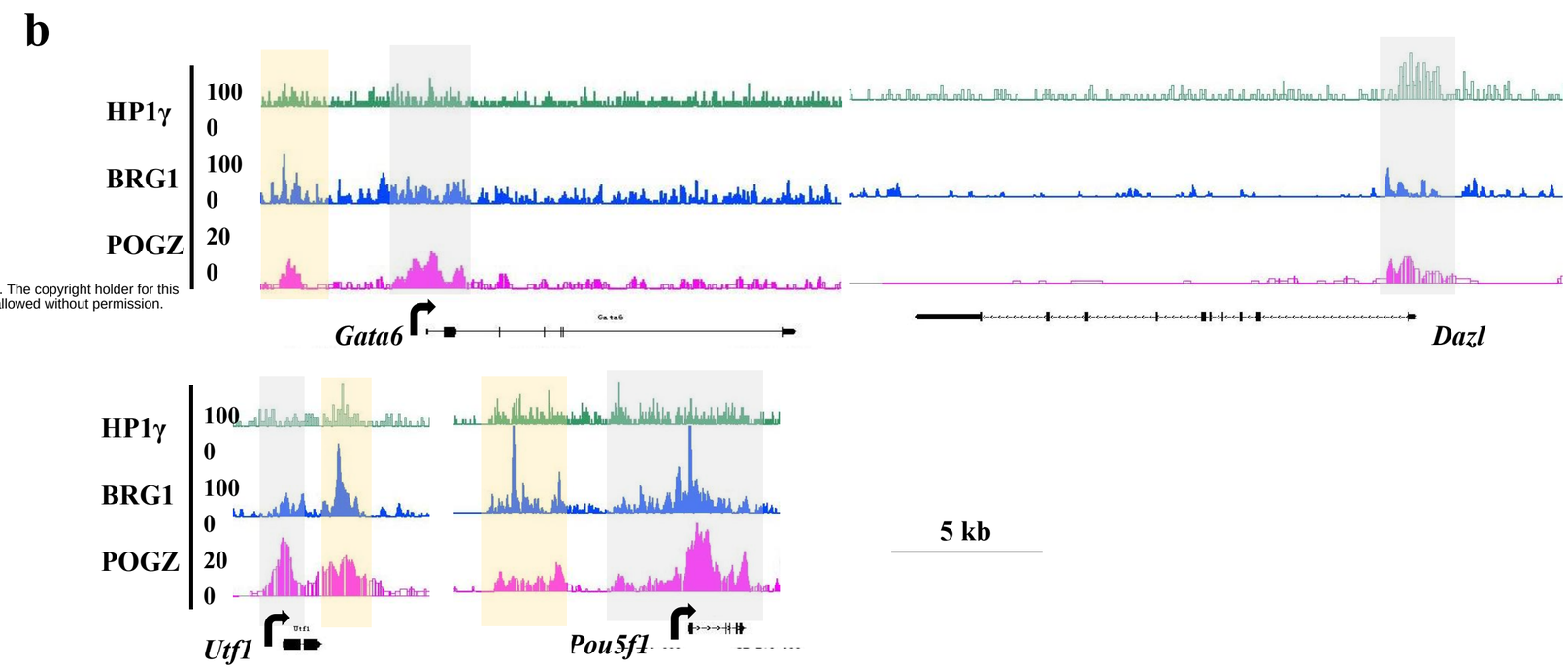

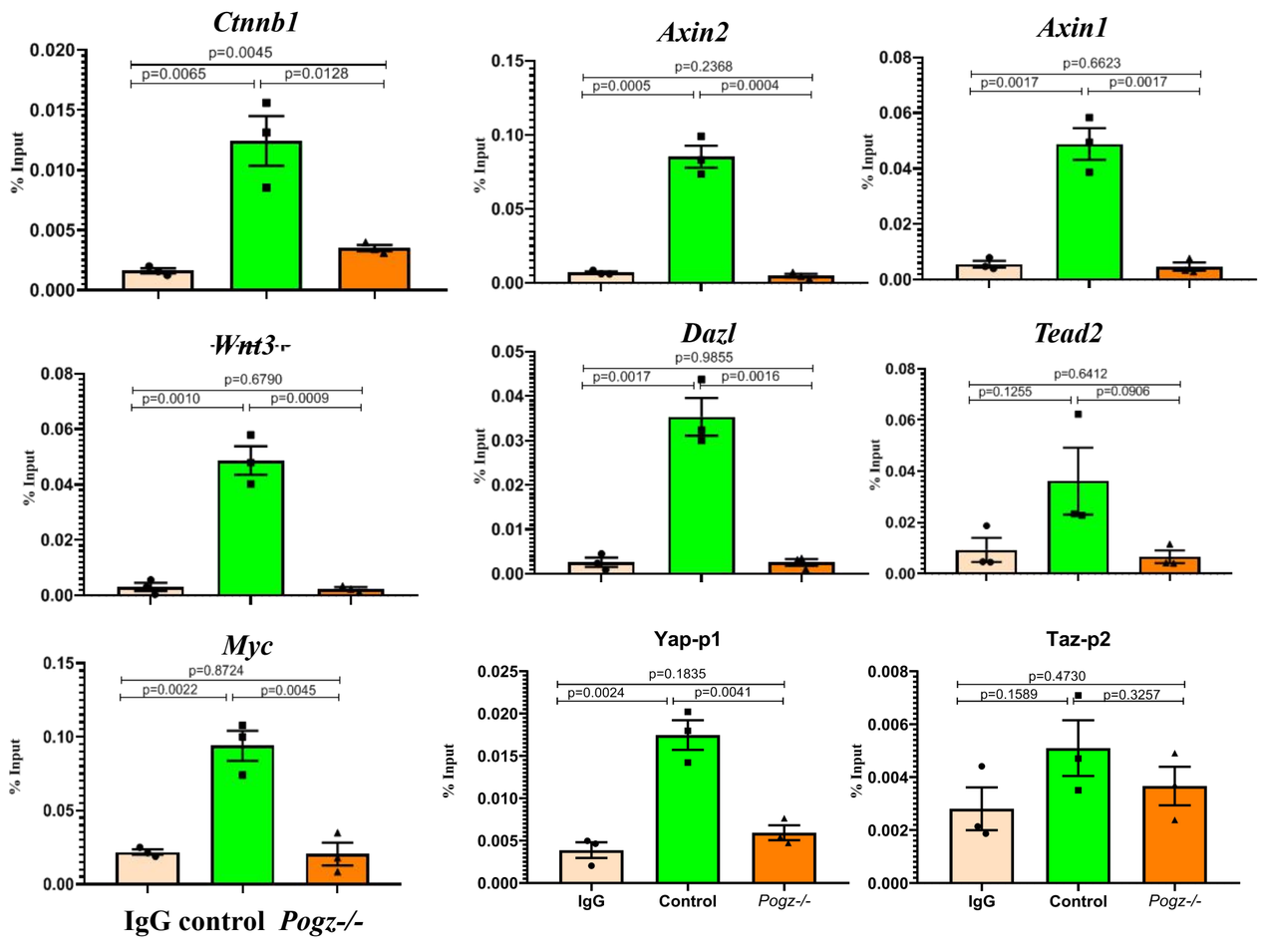

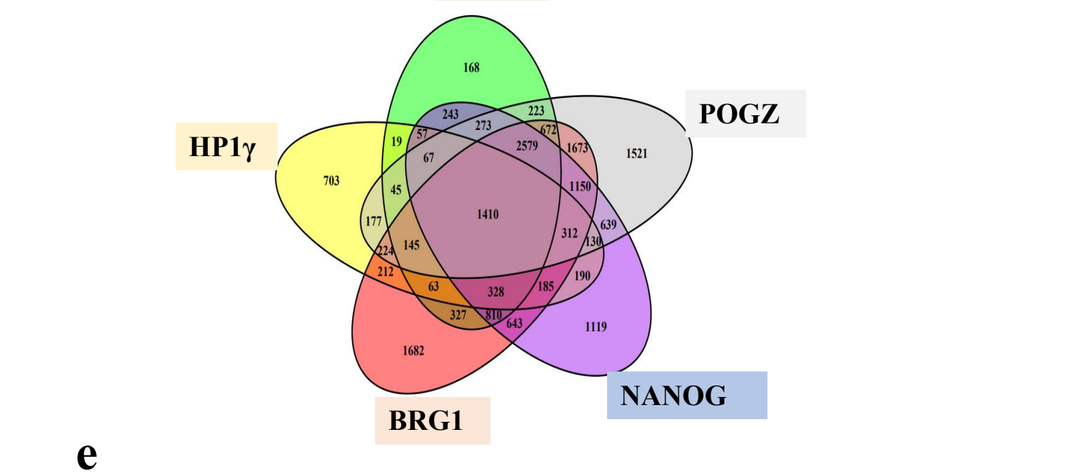

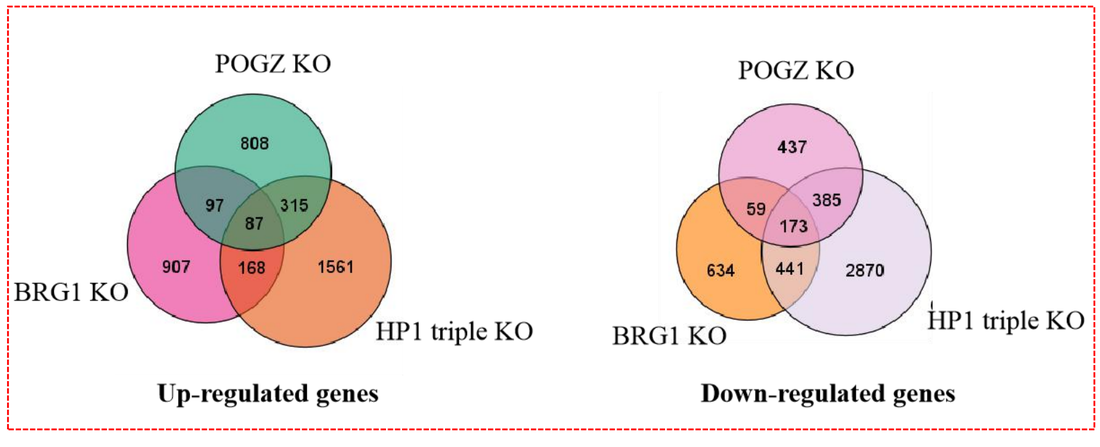

f

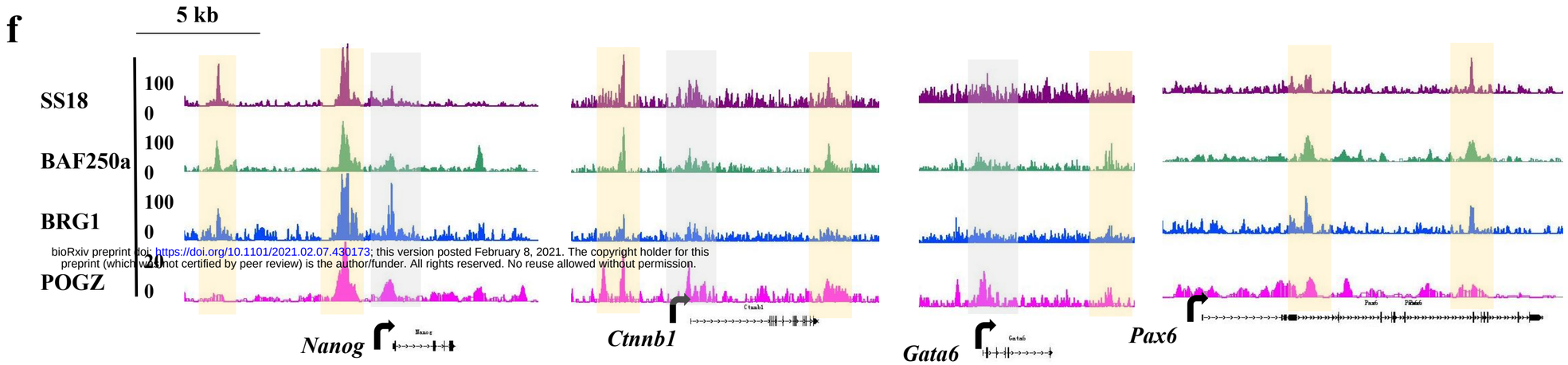

g

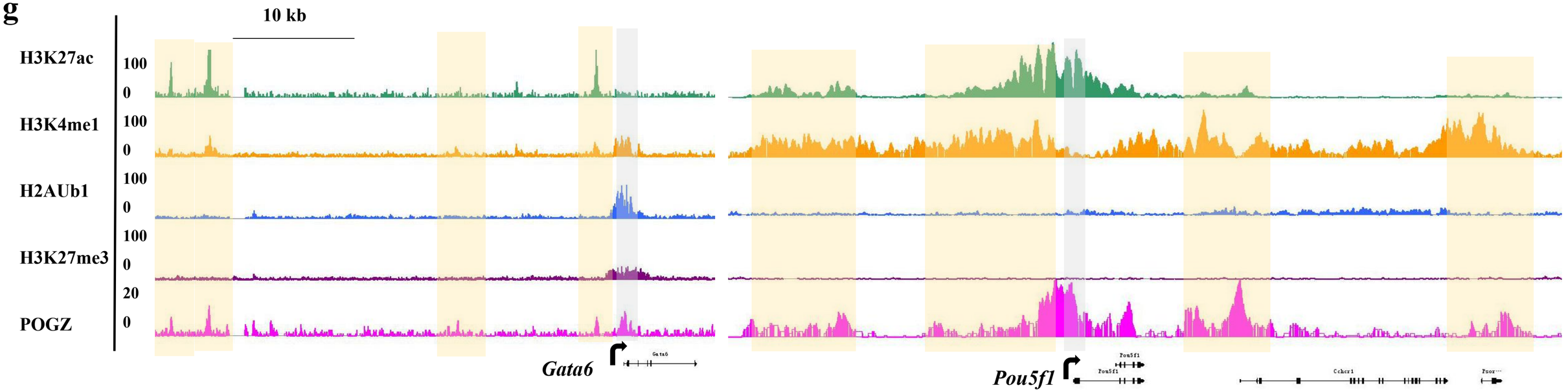

Figure 6 POGZ regulates chromatin accessibility by association with BRG1

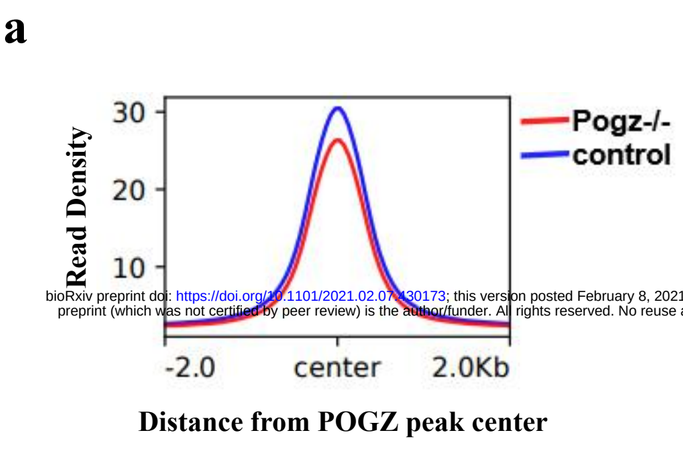

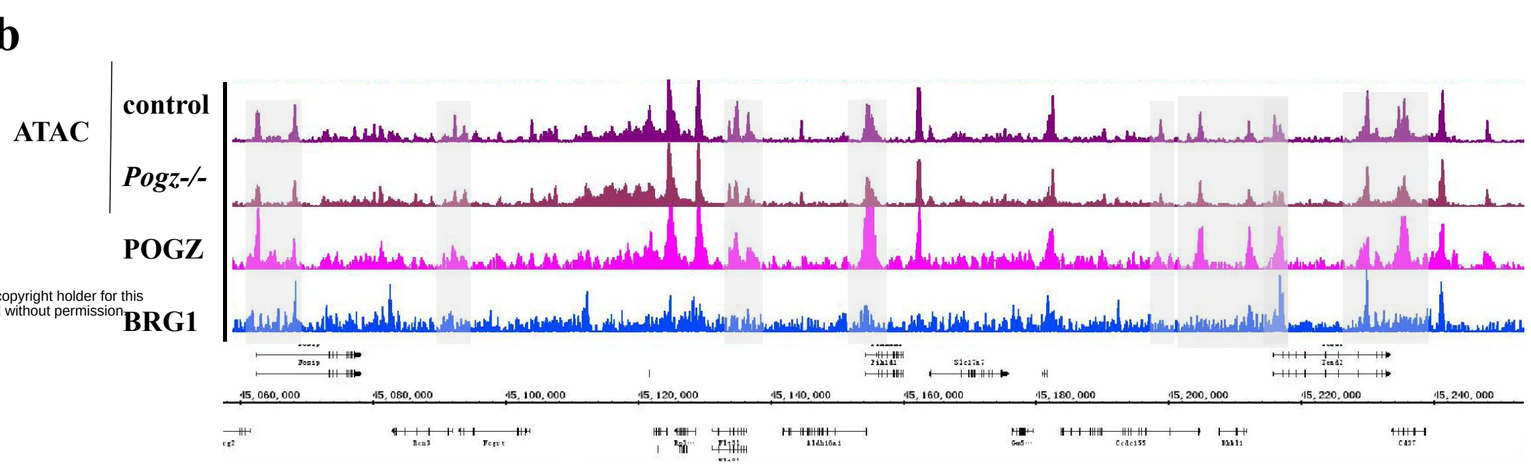

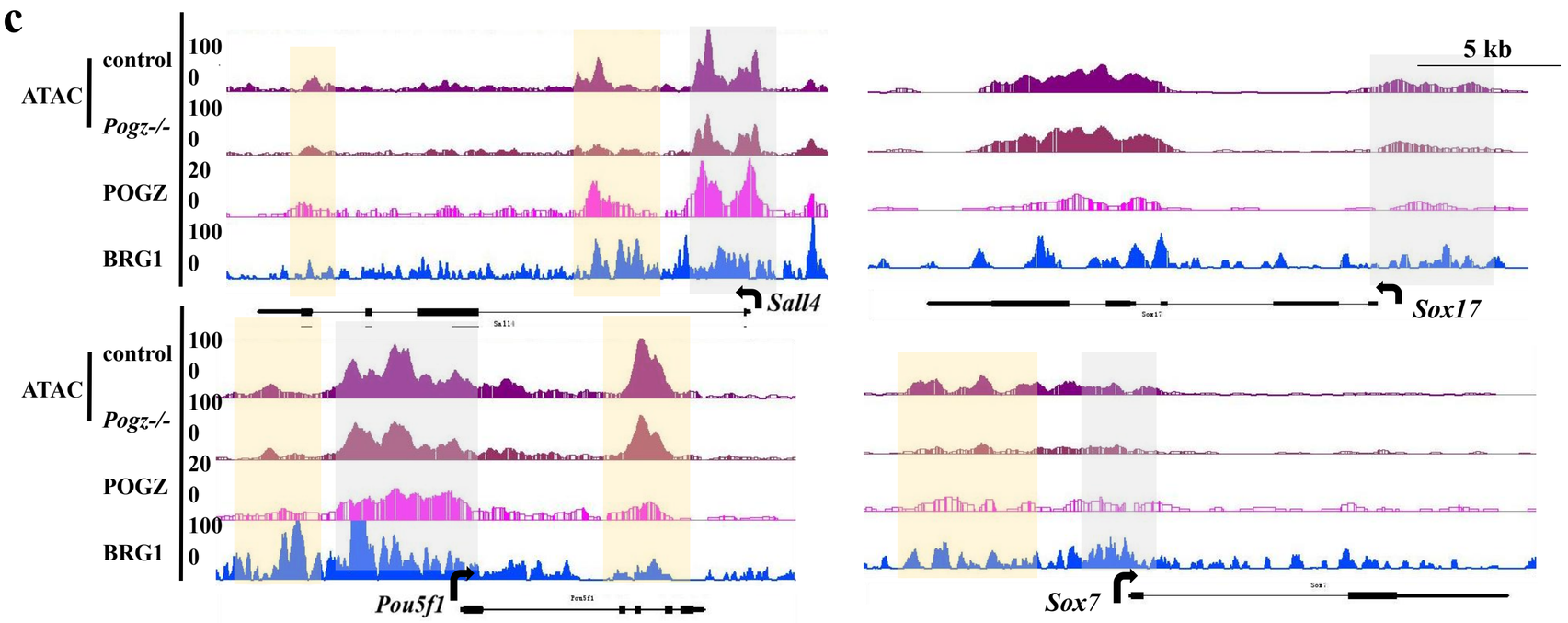

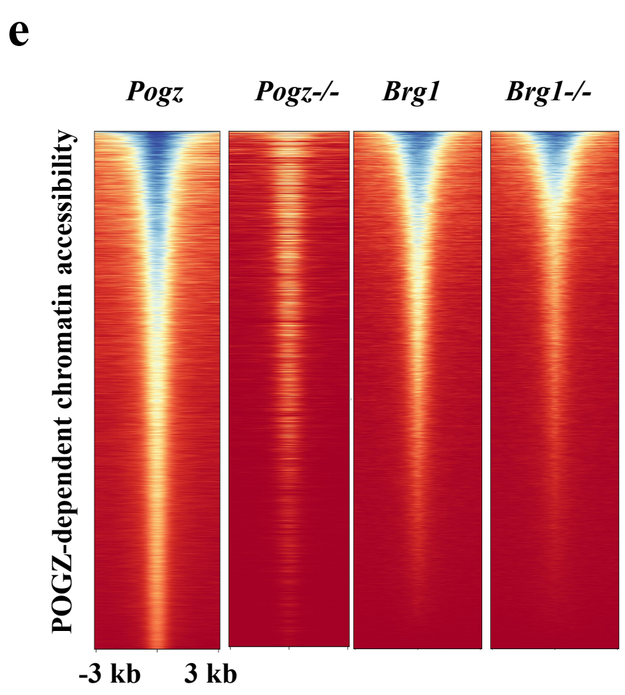

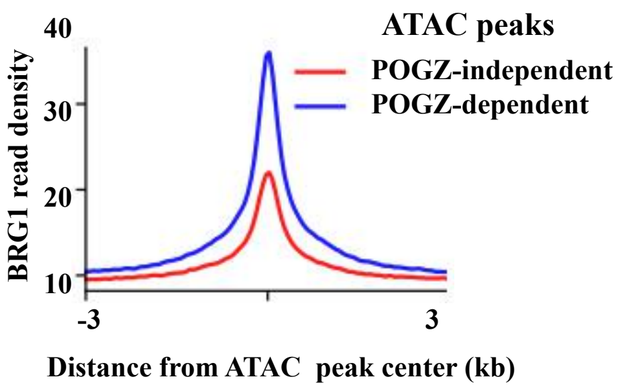

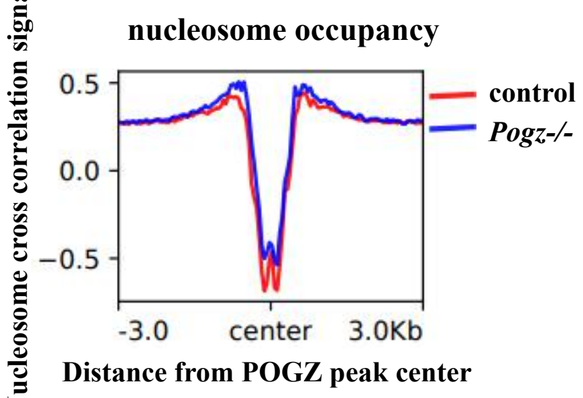

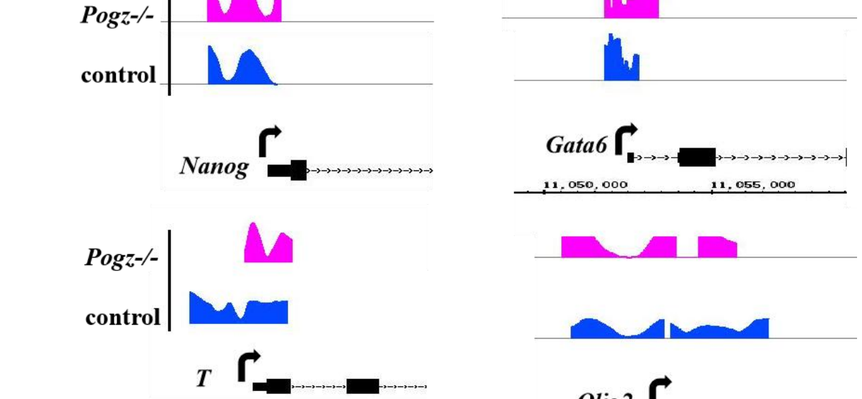

h

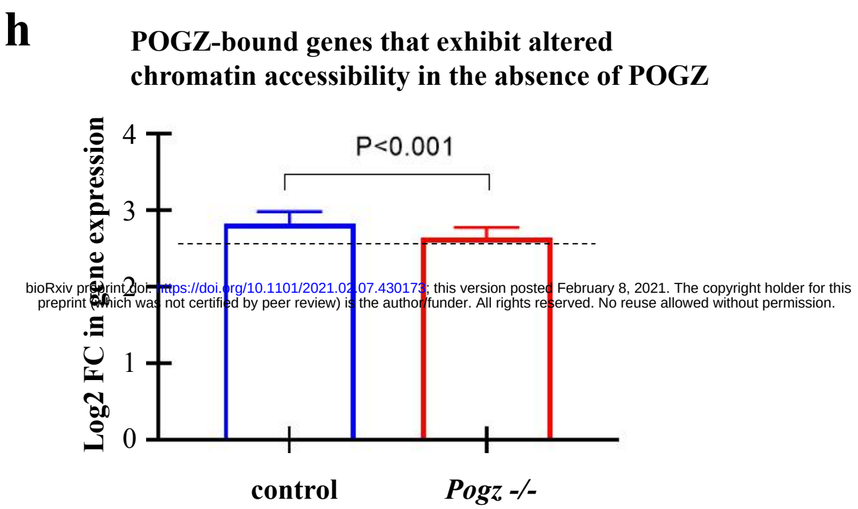

i

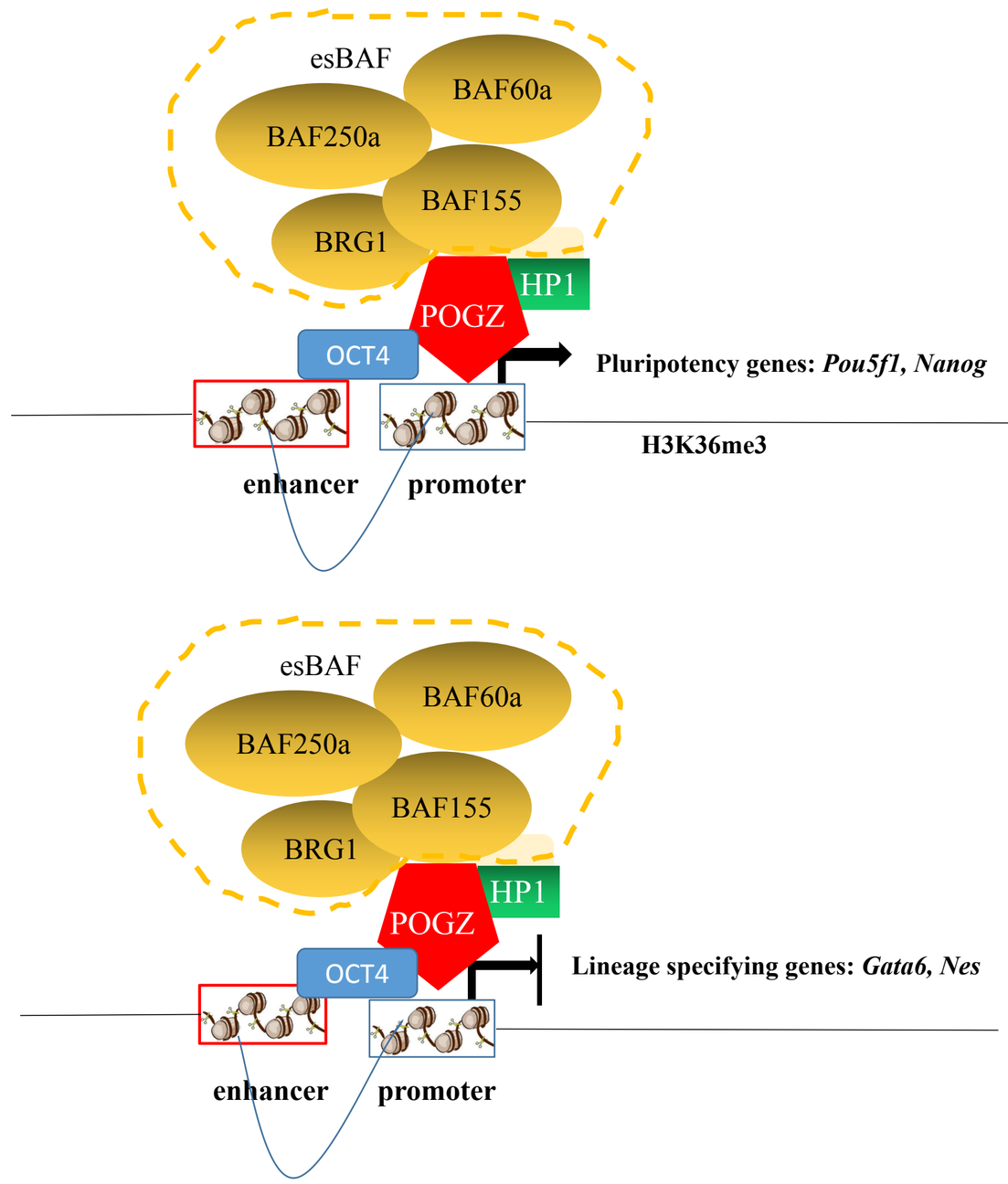

Supplementary Figure 6

a

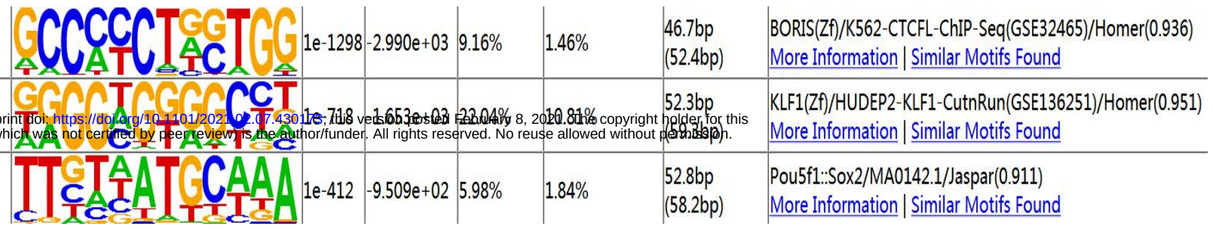

1		1e-1298	-2.990e+03	9.16%	1.46%	46.7bp (52.4bp)	BORIS(Zf)/K562-CTCFL-ChIP-Seq(GSE32465)/Homer(0.936) More Information | Similar Motifs Found
2		1e-718	-1.653e+03	22.04%	10.81%	52.3bp (50.3bp)	KLF1(Zf)/HUDEP2-KLF1-CutnRun(GSE136251)/Homer(0.951) More Information | Similar Motifs Found
3		1e-412	-9.509e+02	5.98%	1.84%	52.8bp (58.2bp)	Pou5f1::Sox2/MA0142.1/Jaspar(0.911) More Information | Similar Motifs Found

b

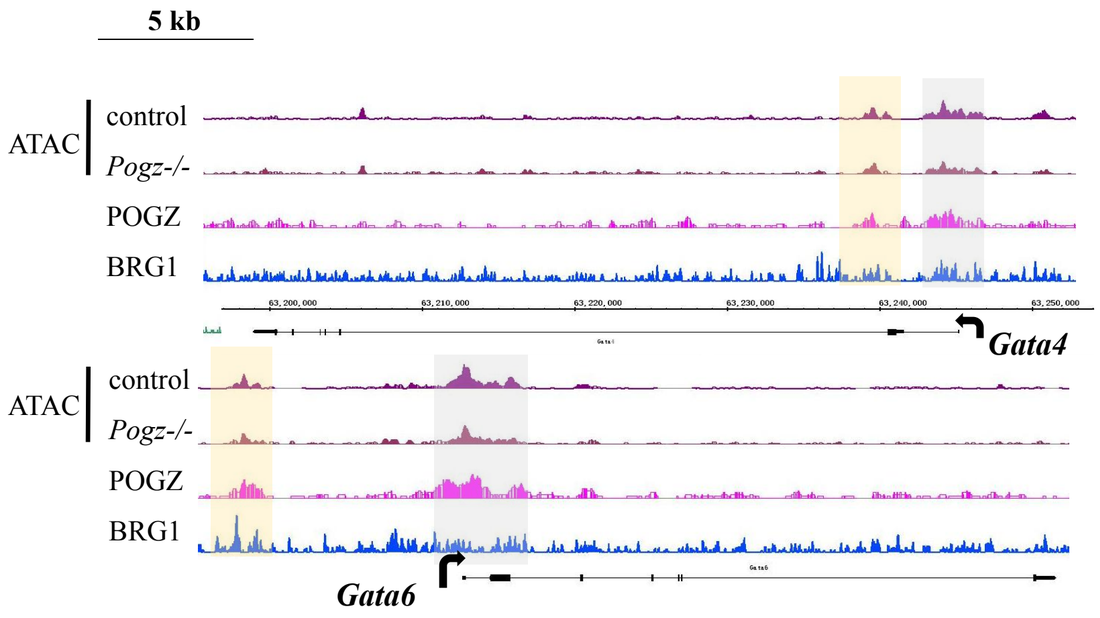

c

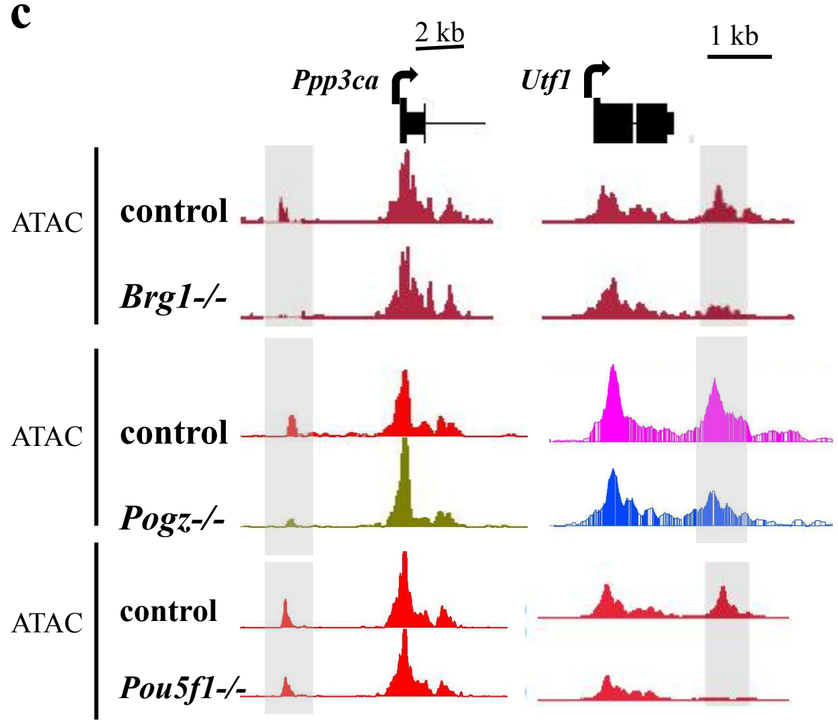

d